Finite volume Galerkin methods for viscous gas dynamics

Ph. Rostand, B. Stoufflet

INRIA

UNITÉ DE RECHERCHE
INRIA-ROCQUENCOURT

Institut National
de Recherche
en Informatique
et en Automatique

Domaine de Voluceau
Rocquencourt
B.P.105
78153 Le Chesnay Cedex
France
Tél.:(1) 39 63 55 11

Rapports de Recherche

N° 863

FINITE VOLUME GALERKIN METHODS FOR VISCOUS GAS DYNAMICS

Philippe ROSTAND
Bruno STOUFFLET

JUILLET 1988

FINITE VOLUME GALERKIN METHODS FOR VISCOUS GAS DYNAMICS

Philippe ROSTAND *

Bruno STOUFFLET **

Abstract :

Finite volume TVD schemes derived for the Euler equations are extended to the Navier-Stokes system. The numerical diffusion introduced in the approximation of the convective part is chosen through a total variation analysis taking in account the physical diffusion. Two dimensional numerical simulations are presented, using a pseudo time dependant implicit algorithm to solve efficiently the steady equations.

METHODES DE VOLUMES FINIS GALERKIN POUR LA DYNAMIQUE DES GAZ VISQUEUX

Résumé :

Un schéma volume finis pour la résolution des équations d'Euler est étendu au cas des équations de Navier-Stokes. La diffusion numérique introduite dans l'approximation du terme de convection est choisie à partir d'une analyse de variation totale, qui prend en compte la diffusion physique. Des simulations numériques bidimensionnelles, obtenues grâce à un algorithme implicite efficace pour le cas stationnaire, sont présentées.

* INRIA-Menusin Domaine de Voluceau Rocquencourt BP 105 78153 Le Chesnay Cedex FRANCE

** AMD-BA 78 Quai Marcel Dassault 92214 Saint Cloud FRANCE

I. INTRODUCTION

Finite volume schemes based on approximate Riemann solver for conservation laws, also called TVD (Total Variation Diminishing) schemes, have received considerable attention in the last twenty years, (see, among others, Harten [10], Van Leer [31], Yee [33]), and can be said to have reached a satisfactory degree of achievement .

These schemes were successfully extended to multidimensional problems, by reducing the equations to one dimension, through the finite volume formulation, and applying the one dimensional techniques. This can be done on unstructured meshes (Baba and Tabata [4], Dervieux [7], Stoufflet-Fezoui [26]).

On the other hand, several research teams have studied such algorithms, on structured meshes, for solving the Navier-Stokes equations. Some 3D codes based on upwind schemes have been developped by Mac Cormack [4], Hänel [25] and Chakravarthy [6], among others.

A particular class of very efficient schemes is that obtained by the combination of a monotone flux formula, and of a second order extension through monotony preserving interpolation, christened Monotonic Upwind Schemes for Conservation Laws (MUSCL) by Van Leer ([32]). These schemes have been derived in order to introduce a "numerical viscosity", which will provide automatic inforcement of the entropy condition, and to provide second order accuracy, at least in regions of regularity.

To solve advection dominated nonlinear parabolic, or incompletely parabolic equations as the compressible Navier-Stokes system, it is necessary to use an approximation which will preserve the entropy condition, but which will also provide sufficient accuracy in viscosity dependant zones, as boundary layers or wakes. In other words, one must make sure that no more diffusion than needed is added.

A model equation for compressible viscous gas dynamics is given by

$$\begin{cases} \dfrac{\partial u}{\partial t} + \dfrac{\partial f(u)}{\partial x} - \epsilon \dfrac{\partial^2 u}{\partial x^2} = 0 \\ u = u(x,t) \in R \end{cases} \tag{1.1}$$

where f is a regular function, not necessarily convex.

In our framework, a numerical scheme to solve (1.1) is made of:

. an approximation of the convection term $\partial f/\partial x$, combining

- a numerical flux function h = h(u,v) with h(u,u) = f(u)
- a MUSCL-like interpolation formula

. an approximation of the diffusion term

. an approximation of the time derivative.

In part II, we will outline the general framework of upwind TVD schemes for multidimensional gas-dynamics equations on triangular (tetrahedral) meshes.

The numerical formulation relying on the approximate Riemann solver proposed by Osher and Chakravarthy [16] and a multidimensional MUSCL like interpolation will be presented. Van Leer, Thomas, Roe and Newsome in [30] have analyzed in one dimension the influence of the choice of the upwind flux formula for the convection part in terms of accuracy, and showed that some flux-vector splitting gave a bad representation of the boundary layer.This will not be our topic; we will only give our arguments in favour of Osher's scheme.

The interpolation, through which second order, or even third order accuracy for one dimensional problems, is reached, is also an important feature of the scheme. In part III, for the one dimensional scalar viscous conservation law (1), we will try to derive conditions on the interpolation which will insure some kind of monotony property, and still allow sufficient accuracy.

In Part IV, we will extend the one dimensional scalar conclusions of Part III to multidimensional systems, taking advantage of the finite volume formulation.

In Part V, we will present different possible time discretizations, including linearly implicit methods, and accelerators for the steady case. This is

an extension of the algorithm proposed by Stoufflet [26] for the inviscid case. Finally, numerical results will be presented and discussed in part VI.

II. GENERAL FRAMEWORK OF THE FINITE VOLUME GALERKIN (FVG) APPROXIMATION

II.1. Mathematical modelling

Let Ω an open set of R^N (N=2 or 3) and let $\Gamma = \partial\Omega$ be its boundary presumed to be smooth. The non-dimensionalized Navier-Stokes equations governing unsteady flows of compressible viscous Newtonian fluids in their conservative form are :

$$\frac{\partial \rho}{\partial t} + \nabla.(\rho u) = 0 \tag{2.1}$$

$$\frac{\partial(\rho u)}{\partial t} + \nabla.(\rho u \otimes u) + \nabla P = \frac{1}{Re}\nabla.(D(u)) \tag{2.2}$$

$$\frac{\partial E}{\partial t} + \nabla.((E+P)u) = \frac{1}{Re}(\nabla.(u.D(u) + \frac{\gamma}{Pr}\nabla T)) \tag{2.3}$$

where

- ρ is the density and T the temperature,
- u is the velocity of the flow,
- P $= (\gamma - 1)\rho T$ is the pressure and E $= \frac{1}{2}\ \rho\ ||u||^2 + \frac{P}{\gamma - 1}$, the total energy
- Re is the Reynolds number and Pr the Prandtl number,
- D(u) is the non-divergent part of the stress tensor:

$$D(u) = \nabla u + \nabla u^t - \frac{2}{3}\nabla.u$$

The left hand side of the equations (1)-(3) constitutes the so-called Euler system of equations governing flows of compressible inviscid fluids.

In the sequel, we consider domains of computation Ω around an obstacle B. Boundary conditions have to be added on the external boundary Γ_∞ and on the wall boundary Γ_B. We denote by n the outward unit normal to Γ.

We assume the flow to be uniform at the infinity, we prescribe :

$$\rho = \rho_\infty, \quad u = u_\infty, \quad P = P_\infty \qquad \text{on } \Gamma_\infty \tag{2.4}$$

On the wall Γ_B we assume the no-slip condition and either the adiabaticity or a given wall temperature :

$$u = 0 \quad \frac{\partial T}{\partial n} = 0 \quad \text{or} \quad T = T_{given} \qquad \text{on } \Gamma_B \tag{2.5}$$

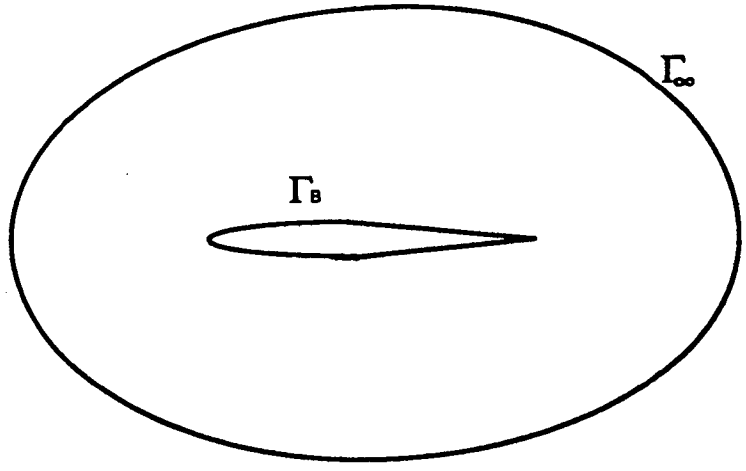

Fig 1

Let W = (ρ, ρu, E) be the vector of conserved quantities ; we can rewrite the system (2.1)-(2.3) as:

$$\frac{\partial W}{\partial t} + \nabla . F(W) = \frac{1}{Re} \nabla . N(W) \tag{2.6}$$

where F and N denote respectively the convective flux term and viscous term.

II.2. General formulation of a variational method

We intend to give a general formulation of a variational method to approximate the system of equations (2.6).

We assume that Ω is a polygonal bounded domain of R^3. Let T_h be a standard tetrahedrization of Ω and h the maximal length of the edges of the tetraedra of T_h.

Let $\mathcal{V}_h$ be a discrete approximation space of continuous, polynomial in each element of T_h scalar functions.

Let $\mathcal{W}_h$ be a discrete approximation space of piecewise continuous scalar functions such that there exists a bijective operator S from $\mathcal{V}_h$ to $\mathcal{W}_h$. (Note that we can have $\mathcal{V}_h = \mathcal{W}_h$, where S would be the identity operator onto $\mathcal{V}_h$)

A general variational approximation involving the two spaces is derived:

$$\begin{cases} \text{Find } W_h \in (\mathcal{V}_h)^n \text{ such that } \forall\ \phi_h \in \mathcal{V}_h, \\ \int_\Omega \frac{\partial W_h}{\partial t}\phi_h dx + \int_\Omega \nabla.(F(W_h)S(\phi_h)dx = \frac{1}{Re}\int_\Omega \nabla.N(W_h)\phi_h dx \end{cases} \tag{2.7}$$

If Γ_g denote the discontinuity surface of a function g $\in \mathcal{W}_h$, and ν its outward unit normal vector, after integration by part, the formulation becomes:

$$\begin{cases} \text{Find } W_h \in (\mathcal{V}_h)^n \text{ such that } \forall\ \phi_h \in \mathcal{V}_h, \\ \quad \int_\Omega \frac{\partial W_h}{\partial t}\phi_h dx + \int_\Omega F(W_h)\nabla(S(\phi_h))dx \\ \quad + \int_{\Gamma_{S(\phi_h)}} F(W_h).\nu[S(\phi_h)]d\sigma + \int_\Gamma F(W_h).nS(\phi_h)d\sigma \\ \quad = -\frac{1}{Re}\int_\Omega N(W_h)\nabla\phi_h dx + \frac{1}{Re}\int_\Gamma N(W_h).n\phi_h d\sigma \end{cases} \tag{2.8a}$$

where [g] represents the jump of the function g through the surface Γ_g.

Another formulation is obtained by a finite volume approximation of the viscous term:

$$
\begin{cases}
\text{Find } W_h \in (\mathcal{V}_h)^n \text{ such that } \forall\ \phi_h \in \mathcal{V}_h, \\
\displaystyle\int_\Omega \frac{\partial W_h}{\partial t}\phi_h dx + \int_\Omega F(W_h)\nabla(S(\phi_h))dx \\
\displaystyle + \quad \int_{\Gamma_{S(\phi_h)}} F(W_h).\nu[S(\phi_h)]d\sigma + \int_\Gamma F(W_h).nS(\phi_h)d\sigma \\
\displaystyle = -\frac{1}{Re}\int_\Omega N(W_h).\nabla S(phi_h)dx + \frac{1}{Re}\int_{\Gamma_{S(\phi_h)}} N(W_h).\nu[S(\phi_h)]d\sigma \\
\displaystyle \quad + \frac{1}{Re}\int_\Gamma N(W_h).nS(\phi_h)d\sigma
\end{cases}
\tag{2.8b}
$$

II.3. Three examples of application

We examine in this section three approximations lying in the space $\mathcal{V}_h$ of continuous, linear in each element, scalar functions. For Euler equations, we will show hereafter that these approximations are equivalent if we suppose that fluxes vary linearly on each element also. Let $\{N_i\}_i$ define the canonical finite element basis of functions of $\mathcal{V}_h$.

i) Consider the complete Galerkin formulation (case where $\mathcal{V}_h = \mathcal{W}_h$, S = identity operator of V_h) that we can find in [2], [13]:

$$
\begin{cases}
\text{Find } W_h \in (\mathcal{V}_h)^n \text{ such that } \forall\ \phi_h \in \mathcal{V}_h, \\
\displaystyle\int_\Omega \frac{\partial W_h}{\partial t}\phi_h dx + \int_\Omega F(W_h)\nabla\phi_h dx + \int_\Gamma F(W_h).n\phi_h d\sigma = R.H.S.
\end{cases}
\tag{2.9}
$$

ii) the second formulation is that proposed by Jameson and al. [14]. The space $\mathcal{W}_h$ is defined by : $\mathcal{W}_h$ is generated by the functions $S(N_i)$, where S is defined below.

Let $\tau(S_i)$ denotes the set of tetrahedra having S_i as a vertex. The construction of the operator S is made as follows:

$$
\forall i, S(N_i) = \frac{1}{3} \text{ on } \bigcup_{T\in\tau(Si)} T \quad \text{and} \quad S(N_i) = 0 \text{ elsewhere.}
$$

The resulting formulation is as follows :

$$\begin{cases} \text{Find } W_h \in (\mathcal{V}_h)^n \text{ such that } \forall\ \phi_h \in \mathcal{V}_h, \\ \int_\Omega \frac{\partial W_h}{\partial t} N_i dx + \sum_{T \in \tau(S_i)} \int_{\partial T} F(W_h).\nu_i d\sigma = R.H.S. \end{cases} \tag{2.10}$$

iii)the third formulation can be found in [27]. The space $\mathcal{W}_h$ is defined as follows:

$$\mathcal{W}_h = \{v_h \in L^\infty(\Omega); v_h = \text{ cste on each cell } C_i, \forall S_i \in \tau_h\}$$

where the cell C_i is the union of the subtriangles having S_i as a vertex and resulting from the subdivision of each triangle of T_h by means of the medians (Fig. 2).

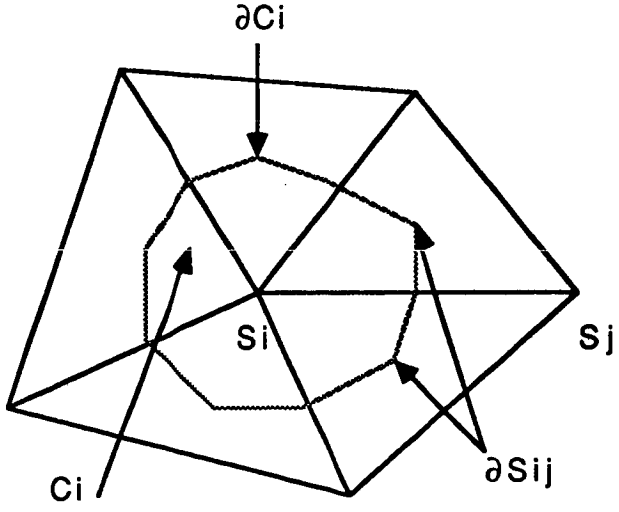

Fig 2

$$\begin{cases} \text{Find } W_h \in (V_h)^n \text{ such that } \forall\ \phi_h \in V_h, \\ \int_\Omega \frac{\partial W_h}{\partial t} N_i dx + \int_{\partial C_i} F(W_h).\nu_i d\sigma + \int_\Gamma F(W_h).n d\sigma = R.H.S \end{cases} \tag{2.11}$$

To show the equivalence in some sense of these formulations, let us consider the case of the Euler equations ($1/Re = 0$), without boundary conditions.

For simplification, we consider the two dimensional case with numerical integration at the midpoints of segments. For each element T $\in T_h$, we denote by indices i,j,k, the quantities evaluated at the vertices S_i, S_j, S_k of T; ∂T_{ij} the face containing vertices S_i and S_j.

Formulation (2.9) becomes:

$$\int_\Omega \frac{\partial W}{\partial t} N_i dx - \sum_{T_i \in \tau(S_i)} \left[F\left(\frac{W_i + W_j}{2}\right) + F\left(\frac{W_i + W_k}{2}\right) + F\left(\frac{W_j + W_k}{2}\right) \right] . \nabla N_i(T) \frac{area(T)}{3} = 0 \tag{2.12}$$

Remarking that we have the identity

$$\nabla N_i(T) + \nabla N_j(T) + \nabla N_k(T) = 0 \tag{2.13}$$

we obtain the equality :

$$\int_\Omega \frac{\partial W}{\partial t} N_i dx = \sum_{T \in \tau_i} \frac{area(T)}{3} \left\{ F\left(\frac{W_i + W_j}{2}\right) . \nabla N_i(T) + F\left(\frac{W_i + W_k}{2}\right) . \nabla N_i(T) - F\left(\frac{W_j + W_k}{2}\right) . \nabla N_j(T) - F\left(\frac{W_j + W_k}{2}\right) . \nabla N_k(T) \right\} \tag{2.14}$$

Formulation (2.10) becomes :

$$\int_\Omega \frac{\partial W}{\partial t} N_i dx - \sum_{T \in \tau(S_i)} \frac{1}{3} F\left(\frac{W_j + W_k}{2}\right) \int_{\partial T_{jk}} n d\sigma = 0 \tag{2.15}$$

We have the geometrical equality in each element :

$$\int_{\partial T_{jk}} n d\sigma = -2 \ area(T) \ \nabla N_i(T) \tag{2.16}$$

and replacing (16) in equality (15), we obtain finally :

$$\int_\Omega \frac{\partial W}{\partial t} N_i dx - \sum_{T \in \tau(S_i)} \frac{2\ area(T)}{3} \left\{ F\left(\frac{W_j + W_k}{2}\right) . \nabla N_j(T) + F\left(\frac{W_j + W_k}{2}\right) . \nabla N_k(T) \right\} = 0 \tag{2.17}$$

Finally, formulation (2.11) becomes:

$$\int_\Omega \frac{\partial W}{\partial t} N_i dx - \sum_{T \in \tau(S_i)} \left[\int_{\partial C_{ij} \cap T} F(W).n d\sigma + \int_{\partial C_{ik} \cap T} F(W).n d\sigma \right] = 0 \tag{2.18}$$

where ∂C_{ij} denotes the two segments of ∂C_i joining at the midpoint of S_i and S_j, as seen on Fig. 3:

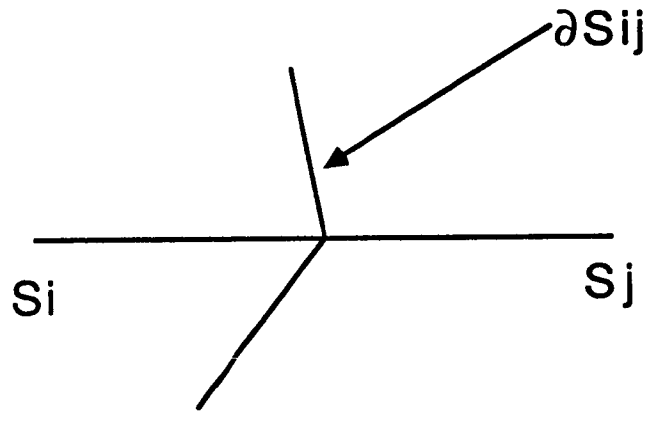

Fig 3

Once again, it is easy to verify that :

$$\int_{\partial C_{ij} \cap T} n d\sigma = \frac{area(T)}{3} [\nabla N_i(T) - \nabla N_j(T)] \tag{2.19}$$

giving the following formulation

$$\left\{ \int_\Omega \frac{\partial W}{\partial t} N_i dx - \sum_{T \in \tau(S_i)} \frac{area(T)}{3} \left\{ F\left(\frac{W_i + W_j}{2}\right) . [\nabla N_i(T) - \nabla N_j(T)] + F\left(\frac{W_i + W_k}{2}\right) . [\nabla N_i(T) - \nabla N_k(T)] \right\} \right. \tag{2.20}$$

Since we suppose that the flux function F varies linearly on each element, we have

$$F\left(\frac{W_{i_1}+W_{i_2}}{2}\right)=\frac{F(W_{i_1})+F(W_{i_2})}{2} \qquad \forall i_1,i_2 \tag{2.21}$$

On the other hand, from (16), the following equality is valid :

$$\sum_{T\in\tau(S_i)} area(T)\nabla N_i(T) = -\frac{1}{2}\sum_{T\in\tau(S_i)}\int_{(\partial T)_i} n d\sigma = 0$$

since the integral of the outward normal n on a closed surface is equal to zero.

All formulations (2.14), (2.17), (2.20) can be rewritten as :

$$\int_\Omega \frac{\partial W}{\partial t}N_i dx - \sum_{T\in\tau(S_i)} 2\frac{area(T)}{3}F(\frac{W_j+W_k}{2}).\nabla N_i(T) = 0 \tag{2.22}$$

This equality is easy to check for formulations (2.14) and (2.17). For the last one, let us consider in details the evaluation of the terms.

If we rewrite (2.20), considering identity (2.21), we obtain :

$$\int_\Omega \frac{\partial W}{\partial t}N_i dx - \sum_{T\in\tau(S_i)} \frac{area(T)}{3} \left\{\frac{F(W_i)}{2}(3\nabla N_i(T)) + F\left(\frac{W_j+W_k}{2}\right)\nabla N_i(T)) - (F(W_j).\nabla N_j(T) + F(W_k).\nabla N_k(T))\right\} = 0$$

which gives:

$$\int_\Omega \frac{\partial W}{\partial t}N_i dx - \sum_{T\in\tau(S_i)} \frac{area(T)}{3}F\left(\frac{W_j+W_k}{2}\right).\nabla N_i(T) + \frac{1}{2}\sum_{T\in\tau(S_i)}\frac{area(T)}{3}(F(W_j).\nabla N_j(T) + F(W_k).\nabla N_k(T)) = 0 \tag{2.23}$$

If we look at the last term, we note that for a given vertex S_j, $F(W_j)$ appears each time S_j is vertex of an element of $\tau(S_i)$, so appears twice. Let T_j and $T_{j'}$ denotes these adjacent elements.

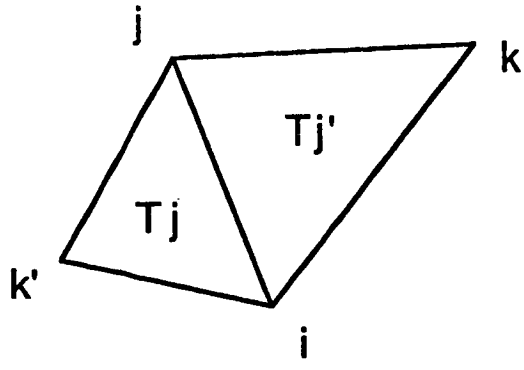

Fig 4

Let S_k and $S_{k'}$ denote the remaining vertices of these elements as in Figure 2.

The last term can be rewritten as :

$$K = \frac{1}{2} \sum_{T \in \tau(S_i)} \frac{area(T)}{3} (F(W_j).\nabla N_j(T) + F(W_k).\nabla N_k(T))$$

$$= \frac{1}{2} \sum_{j \in K(i)} \left\{ \frac{area(T_j)}{3} (F(W_j).\nabla N_j(T_j) + \frac{area(T'_j)}{3} (F(W_j).\nabla N_j(T'_j) \right\}$$

$$= \frac{1}{2} \sum_{T \in K(i)} \left\{ F(W_j) \left(-\frac{area(T_j)}{3} \nabla N_i(T_j) - \frac{area(T'_j)}{3} \nabla N_i(T'_j)) \right) \right.$$

$$\left. + F(W_j) \left(-\frac{area(T_j)}{3} \nabla N_k(T_j) - \frac{area(T'_j)}{3} \nabla N'_k(T'_j) \right) \right\}$$

But, we know that

$$-\frac{area(T_j)}{3} \nabla N_k(T_j) - \frac{area(T'_j)}{3} \nabla N_{k'}(T'_j)$$

$$= \frac{1}{2} \int_{(\partial T j)_k} n d\sigma - \frac{1}{2} \int_{(\partial T_{j'})_{k'}} n d\sigma = 0$$

It gives :

$$K = \frac{1}{2} \sum_{j \in K(i)} F(W_j)(-\frac{area(T_j)}{3} \nabla N_i(T_j) - \frac{area(T'_j)}{3} \nabla N_i(T'_j))$$

$$= \sum_{T \in K(i)} -\frac{area(T)}{3} \left[\frac{F(W_j) + F(W_k)}{2} \right] \nabla N_i(T)$$

Reporting expression K (in (2.23), we obtain equality (2.22).

This shows the equivalence of the three formulations in the inviscid linear case.

Similarly, we can show the equivalence of the two approximations in the viscous case, when the diffusion operator N is linear. Nevertheless, significant differences appear in the non linear case, or when upwinding is introduced.

II.4. Upwind formulation for the Navier-Stokes equations

We return to the third formulation (2.11) that we will use in the sequel with the alternate approximation of the R.H.S. given in (2.8b).

The numerical integration of the viscous terms of the RHS is carried out in a centered way.

The scheme will be completely defined if we precise now which approximation is used to compute the left hand-side integral in (2.11).

Let us introduce the following notations :

$$\begin{aligned} F_{ij}(U) &= F(U).\int_{\partial S_{ij}} \nu_i d\sigma \\ P_{ij}(U) &= F_1'(U).\int_{\partial S_{ij}} \nu_{ix} d\sigma + F_2'(U)\int_{\partial S_{ij}} \nu_{iy} d\sigma \\ &= \nabla.F(U).\int_{\partial Sij} \nu_i d\sigma \end{aligned}$$

Problem (2.11) has the following formulation:

$$\left\{ \begin{array}{l} \text{Find } W_h \in (V_h)^m, \\ \displaystyle\int_\Omega \frac{\partial W_h}{\partial t} N_i dx + \sum_{j\in\kappa(i)} \int_{\partial S_{ij}} F(W_h).\nu_i d\sigma + \int_{\partial S_i \cap \Gamma_b} F(W_h).n d\sigma \\ \displaystyle + \int_{\partial S_i \cap \Gamma_\infty} F(W_h).n d\sigma = \frac{1}{Re}\int_{\partial C_i} N(W_h).\nu_i + \frac{1}{Re}\int_\Gamma N(W_h).n d\sigma \end{array} \right. \tag{2.24}$$

Upwinding is introduced in the computation of the convection term through the numerical flux function Φ of a first-order accurate upwind scheme by :

$$\int_{\partial S_{ij}} F(W_h).\nu_i d\sigma = H_{ij}^{(1)} = \Phi_{F_{ij}}(W_i, W_j)$$

where $W_i = W_h(S_i)$ and $W_j = W_h(S_j)$.

The numerical flux function used in this study is the Osher approximate Riemann solver [15]:

$$\Phi_{Fij}^{OS}(U,V) = \frac{1}{2}(F_{ij}(U) + F_{ij}(V)) - \frac{1}{2}\int_U^V |P_{ij}(W)|dW \qquad (2.25)$$

where the integral is carried out along a path piecewise parallel to the eigenvectors of $P_{ij}(U)$.

The numerical integration with the upwind scheme, as described previously, leads to approximations which are only first-order accurate. We present a second-order accurate MUSCL-like extension without changing the approximation space:

$$\begin{cases} \text{Find } W_h \in (V_h)^m \\ \int_{C_i} \frac{\partial W_h}{\partial t} dx + \sum_{j\in\kappa(i)} H_{ij}^{(2)} + \int_{\partial C_i \cap \Gamma_b} F(W_h).n d\sigma \\ \qquad + \int_{\partial C_i \cap \Gamma_\infty} F(W_h).n d\sigma = R.H.S. \end{cases} \qquad (2.3)$$

where

$$H_{ij}^{(2)} = \Phi_{F_{ij}}(W_{ij}, W_{ji}).$$

The arguments W_{ij} and W_{ji} are values at the interface ∂S_{ij} interpolated using upwinded gradients as described below.

We define the downstream and upstream triangles T_{ij} and T_{ji} for each segment S_iS_j as shown in Fig. 5.

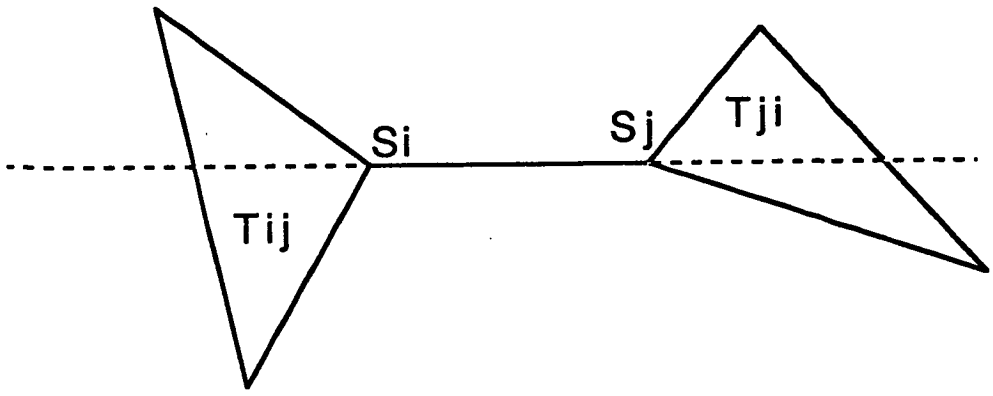

Fig 5

Let the centered gradient be (Fig 3):

$$\nabla W_{ij} = \nabla W|_{T^1_{ij}} = \nabla W|_{T^2_{ij}}$$

The values at interface needed to compute the flux $H^{(2)}_{ij}$ are now given by :

$$\begin{cases} W_{ij} = W_i + L_{ij} \left(\frac{1-\kappa}{4}\nabla W|_{T_{ij}} + \frac{1+\kappa}{4}\nabla W_{ij}\right).S_iS_j \\ W_{ji} = W_j - L_{ji} \left(\frac{1-\kappa}{4}\nabla W|_{T_{ji}} + \frac{1+\kappa}{4}\nabla W_{ij}\right).S_iS_j \end{cases} \tag{2.4}$$

where the parameter κ can be chosen to select the degree of upwinding in the interpolation and L_{ij} and L_{ji} are the limiting matrices, which are introduced to reduce numerical oscillations of the solution and to provide some kind of monotonicity property.

A good procedure in term of accuracy is to use limiters on characteristic variables. For this, we compute these variables by the transformation taken at midpoint of the segment. If we denote by Π_{ij} the transformation matrix corresponding to $P_{ij}(W(\frac{S_i+S_j}{2}))$, the values at interface are now given by :

$$\begin{cases} W_{ij} = W_i + \Pi_{ij} Lc_{ij} \Pi^{-1}_{ij} \left(\frac{1-\kappa}{4}\nabla W|_{T_{ij}} + \frac{1+\kappa}{4}\nabla W_{ij}\right).S_iS_j \\ W_{ji} = W_j - \Pi_{ij} Lc_{ji} \Pi^{-1}_{ij} \left(\frac{1-\kappa}{4}\nabla W|_{T_{ij}} + \frac{1+\kappa}{4}\nabla W_{ji}\right).S_iS_j \end{cases} \tag{2.5}$$

where Lc_{ij} and Lc_{ji} are diagonal matrices.

II.3 Boundary conditions

Wall boundary :

The no-slip boundary condition and the given wall temperature are imposed strongly. This is an advantage of such a vertex centered approximation. No pressure extrapolation is carried out.

Inflow and outflow boundaries :

At these boundaries we suppose the flow to be advection dominated, and so we have to select a precise set of compatible exterior datas, depending on the flow regime and the direction of velocity. For this purpose, a plus-minus flux splitting is applied between exterior datas and interior values. More precisely, the inviscid part of the boundary integral is evaluated with the use of the following flux-splitting

$$\int_{\partial C_i \cap \Gamma_\infty} F(W_h).n d\sigma = P^+_{i\infty}(W_i)W_i + P^-_{i\infty}(W_i)W_\infty$$

where

$$P_{i\infty}(W) = F'(W).\int_{\partial C_i \cap \Gamma_\infty} n d\sigma$$

III. ONE DIMENSIONAL SCALAR ANALYSIS.

We first consider a one-dimensional scalar conservation-diffusion law :

$$\begin{cases} \dfrac{\partial u}{\partial t} + \dfrac{\partial}{\partial x} f(u) - \epsilon \dfrac{\partial^2 u}{dx^2} = 0 \\ u = u(x,t), \qquad \epsilon > 0 \end{cases} \tag{3.1}$$

f is a real function, not necessarily convex.

We define a regular mesh and apply the finite volume scheme defined in section II to (3.1).

We denote by h the mesh size, by x_j = jh , j $\in$ Z, $u_j = u(x_j)$.

The i th equation is

$$\left\{\begin{array}{l} \dfrac{\partial u_j}{\partial t}+ \\ \dfrac{1}{h}\Big[\ \Phi(\ u_j+\dfrac{r_j}{4}((1-\kappa)(u_j-u_{j-1})+(1+\kappa)(u_{j+1}-u_j))\ , \\ \qquad u_{j+1}-\dfrac{l_{j+1}}{4}((1-\kappa)(u_{j+2}-u_{j+1})+(1+\kappa)(u_{j+1}-u_j))\ ) \\ \quad -\Phi(\ u_{j-1}+\dfrac{r_{j-1}}{4}((1-\kappa)(u_{j-1}-u_{j-2})+(1+\kappa)(u_j-u_{j-1}))\ , \\ \qquad u_j-\dfrac{r_j}{4}((1-\kappa)(u_{j+1}-u_j)+(1+\kappa)(u_j-u_{j-1}))\ )\ \Big] \\ -\dfrac{\epsilon}{h^2}(u_{j+1}-2u_j+u_{j-1}) \qquad =0 \end{array}\right. \tag{3.2}$$

For simplicity, we have denoted by r_i (resp. l_i) the right limiter $L_{i,i+1}$ (resp. the left limiter $L_{i,i-1}$).

The numerical flux function Φ verifies $\Phi(u,u) = \mathrm{f(u)}$; it will be supposed to be monotone, i.e. $\Phi(v,w)$ is a non increasing function of w and a non decreasing function of v. For example, Φ can be the Enquist-Osher flux formula ([8],[9]):

$$\phi(v,w) = \frac{f(v)+f(w)}{2} - \frac{1}{2}\int_v^w |f'(x)|dx \tag{3.3}$$

but our study is more general.

The scheme (3.2) is defined by two parameters: the right and left slope limiters, and the parameter κ defining the extrapolation. Note that the slope limiters r_i and l_i are different. However, if one wants to have the same treatment of forward and backward discontinuities, r_i and l_i must be linked, see equation (3.25).

The purpose of slope limiting is to provide some kind of monotony or TVD property [10] ; it has received considerable attention in the recent years [28], [16], [32], [29]. However, all these studies are designed for the inviscid ($\epsilon = 0$) equation. Our point is to derive a condition for total variation diminishing taking in account the physical diffusion term $\epsilon\partial^2 u/\partial x^2$.

Following Osher [15], Osher and Chakravarty [16], Harten [10], Sanders [24], we will write our five point scheme as

$$\frac{du_j}{dt} - C_{j+\frac{1}{2}}\Delta^+ u_j + D_{j-\frac{1}{2}}\Delta u_j = 0 \tag{3.4}$$

where

$$\Delta^+ u_j = u_{j+1} - u_j \tag{3.5.a}$$

$$\Delta^- u_j = u_j - u_{j-1} \tag{3.5.b}$$

$$C_{j+\frac{1}{2}} = C_{j+\frac{1}{2}}(u_{j+2}, u_{j+1}, u_j, u_{j-1})$$

$$D_{j-\frac{1}{2}} = D_{j-\frac{1}{2}}(u_{j+1}, u_j, u_{j-1}, u_{j-2})$$

The following result, due to Osher, Chakavarthy and Sanders, will be our starting point.

Theorem 1 :

$$\text{If} \quad \begin{cases} C_{j+\frac{1}{2}} \geq 0 \\ D_{j-\frac{1}{2}} \geq 0 \end{cases} \quad \text{then} \quad \frac{d}{dt}TV(u) \leq 0$$

where $TV(u)$ is the total variation of u.

Proof :

$$TV(u) = \frac{1}{h}\sum_j |u_{j+1} - u_j| = \frac{1}{h}\sum_j \alpha_j \Delta^+ u_j$$

$$\text{where} \quad \alpha_j = \begin{cases} 1 \text{ if } \Delta^+ u_j \geq 0 \\ -1 \text{ if } \Delta^+ u_j < 0 \end{cases}$$

$$\begin{aligned} &\frac{d}{dt}TV(u) \\ &= \frac{1}{h}\sum_j \alpha_j \frac{d}{dt}\Delta^+ u_j \\ &= \frac{1}{h}\sum_j \alpha_j \left[C_{j+\frac{3}{2}}\Delta^+ u_{j+1} - (D_{j+\frac{1}{2}} + C_{j+\frac{1}{2}})\Delta^+ u_j + D_{j+\frac{1}{2}}\Delta^+ u_{j-1}\right] \\ &= \frac{1}{h}\sum_j \left[(\alpha_{j-1} - \alpha_j)C_{j+\frac{1}{2}} + (\alpha_{j+1} - \alpha_j)D_{j+\frac{1}{2}}\right]\Delta^+ u_j \end{aligned}$$

$$\frac{d}{dt}TV(u) \leq 0$$

because

$$(\alpha_{j-1} - \alpha_j)\Delta^+ u_j \leq 0 \qquad \text{and} \qquad (\alpha_{j+1} - \alpha_j)\Delta^+ u_j \leq 0$$

$(\Diamond)$

Following Osher [15], we find from (3.2) that :

$$\begin{aligned} C_{j+\frac{1}{2}} = \frac{1}{h}\Big[& \Phi\big(u_j + \tfrac{r_j}{4}((1-\kappa)\Delta^- u_j + (1+\kappa)\Delta^+ u_j), \\ & \quad u_{j+1} - \tfrac{l_{j+1}}{4}((1-\kappa)\Delta^+ u_{j+1} + (1+\kappa)\Delta^- u_{j+1}) \big) \\ & -\Phi\big(u_j + \tfrac{r_j}{4}((1-\kappa)\Delta^- u_j + (1+\kappa)\Delta^+ u_j), \\ & \quad u_j - \tfrac{l_j}{4}((1-\kappa)\Delta^+ u_j + (1+\kappa)\Delta^- u_j) \big) \Big] \quad \frac{-1}{\Delta^+ u_j} \\ & + \frac{\epsilon}{h^2} \end{aligned} \tag{3.6}$$

$$\begin{aligned} D_{j-\frac{1}{2}} = \frac{1}{h}\Big[& \Phi\big(u_j + \tfrac{r_j}{4}((1-\kappa)\Delta^- u_j + (1+\kappa)\Delta^+ u_j), \\ & \quad u_j - \tfrac{l_j}{4}((1-\kappa)\Delta^+ u_j + (1+\kappa)\Delta^- u_j) \big) \\ & -\Phi\big(u_{j-1} + \tfrac{r_{j-1}}{4}((1-\kappa)\Delta^- u_{j-1} + (1+\kappa)\Delta^+ u_{j-1}), \\ & \quad u_j - \tfrac{l_j}{4}((1-\kappa)\Delta^+ u_j + (1+\kappa)\Delta^- u_j) \big) \Big] \quad \frac{1}{\Delta^- u_j} \\ & + \frac{\epsilon}{h^2} \end{aligned} \tag{3.7}$$

For a Lipschitz continuous flux ϕ, we will define a local Peclet number by:

$$\nu_i = \frac{a_i h}{2\epsilon} \tag{3.8}$$

where a_i is the Lipschitz norm of ϕ in a neighborhood I_i of u_i of chosen size,

i.e.

$$a_i = \text{Max}\left\{\sup_{x\in I_i}\left(\sup_{\substack{y,z\in I_i\\ y\neq z}}\frac{\phi(y,x)-\phi(z,x)}{y-z}\right),\right.$$
$$\left.\sup_{x\in I_i}\left(\sup_{\substack{y,z\in I_i\\ y\neq z}}\frac{\phi(x,y)-\phi(x,z)}{y-z}\right)\right\}$$

$a_i \geq 0$ because of the monotony of the flux function Φ.

Note that if the equation is linear, i.e.

$$f(u) = au \tag{3.10}$$

then

$$\phi(v,w) = a^+v + a^-w \tag{3.11}$$

where

$$a^{\pm} = \frac{a \pm |a|}{2} \tag{3.12}$$

and

$$a_i = |a| \tag{3.13}$$

and the definition of the Peclet Number is the usual one.

Going back to the general case, we denote by

$$\delta_j = \frac{\Delta^+ u_j}{\Delta^- u_j} \tag{3.14}$$

and we take

$$I_j = (u_j - k\Delta^- u_j, u_j + k\Delta^+ u_j) \tag{3.15}$$

where k is a chosen positive parameter.

The limiters r and l are taken to be functions of δ, as usual.

$$r_j = r_j(\delta_j) \qquad l_j = l_j(\delta_j)$$

We have the following result:

Theorem 2. Let $\theta \in [0,1]$.

If When $\delta_j \geq 0$ or $\delta_j \leq \dfrac{\kappa-1}{1+\kappa}$

$$0 \leq r_j \leq \frac{4 \ \inf\left(k, \theta(1+1/2\nu_j)\right)\delta_j}{(1-\kappa)+(1+\kappa)\delta_j} \tag{3.16}$$

When $\delta_j \leq \dfrac{\kappa-1}{1+\kappa}$

$$0 \leq r_j \leq \frac{4 \ \inf\left((k-1), (1-\theta)(1+1/2\nu_{j-1})\right)}{(\kappa-1)-(1+\kappa)\delta_j} \tag{3.17}$$

and When $\delta_j \geq \dfrac{1+\kappa}{\kappa-1}$

$$0 \leq l_j \leq \frac{4 \ \inf\left(k, \theta(1+1/2\nu_{j+1})\right)}{(1-\kappa)\delta_j+(1+\kappa)} \tag{3.18}$$

When $\dfrac{1+\kappa}{\kappa-1} \leq \delta_j \leq 0$

$$0 \leq l_j \leq \frac{4 \ \inf\left((k-1), (1-\theta)(1+1/2\nu_j)\right)\delta_j}{(\kappa-1)\delta_j-(1+\kappa)} \tag{3.19}$$

then $C_{j+\frac{1}{2}}$ and $D_{j+\frac{1}{2}}$ are positive numbers; the scheme defined in (3.1) is T.V.D.

θ is a chosen parameter; with $\theta < 1$, one can avoid the necessity to put the limiter to zero at extremas.

Proof :

We will prove the result for $D_{j-\frac{1}{2}}$, the demonstration for $C_{j+\frac{1}{2}}$ is absolutely similar.

$$hD_{j-\frac{1}{2}} =$$

$$\frac{1}{\Delta^- u_j}\Bigg[\Phi\left(u_j + \frac{r_j}{4}\left[(1-\kappa)\Delta^- u_j + (1+\kappa)\Delta^+ u_j\right] \ , \ v_j\right)$$

$$-\Phi\left(u_{j-1} + \frac{r_{j-1}}{4}\left[(1-\kappa)\Delta^- u_{j-1} + (1+\kappa)\Delta^+ u_{j-1}\right] \ , \ v_j\right)\Bigg]$$

$$+\frac{\epsilon}{h}$$

$$\text{where} \quad v_j = u_j - \frac{l_j}{4}\left((1-\kappa)\Delta^+ u_j + (1+\kappa)\Delta^- u_j\right)$$

Using (3.18) and (3.19), it is easy to see that $v_j \in I_{j-1}$.

Let us suppose that $\Delta^- u_j = \Delta^+ u_{j-1} \geq 0$, then from (3.16)

$$\begin{aligned} u_{j-1} + \frac{r_{j-1}}{4}\left[(1-\kappa)\Delta^- u_{j-1} + (1+\kappa)\Delta^+ u_{j-1}\right] \\ \leq\ u_{j-1} + \theta\left(1 + \frac{1}{2\nu_{j-1}}\right)(u_j - u_{j-1}) \end{aligned} \tag{3.20}$$

by (3.17)

$$u_j + \frac{r_j}{4}\left[(1-\kappa)\Delta^- u_j + (1+\kappa)\Delta^+ u_j\right] \geq\ u_j - (1-\theta)\left(1 + \frac{1}{2\nu_{j-1}}\right)(u_j - u_{j-1}) \tag{3.21}$$

$$\begin{aligned} \text{If}\quad u_{j-1} + \frac{r_{j-1}}{4}\left[(1-\kappa)\Delta^- u_{j-1} + (1+\kappa)\Delta^+ u_{j-1}\right] \\ \leq\ u_j + \frac{r_j}{4}\left[(1-\kappa)\Delta^- u_j + (1+\kappa)\Delta^+ u_j\right] \end{aligned} \tag{*}$$

then using the monotony of ϕ and the positivity of ϵ, we have $D_{j-\frac{1}{2}} \geq 0$.

If not, we use the Lipschitz continuity of ϕ with respect to its first variable. Using (3.16)

$$u_{j-1} + \frac{r_{j-1}}{4}\left[(1-\kappa)\Delta^- u_{j-1} + (1+\kappa)\Delta^+ u_{j-1}\right] \in I_{j-1} \tag{3.22}$$

$$\begin{aligned} \text{as}\quad u_j + \frac{r_j}{4}\left[(1-\kappa)\Delta^- u_j + (1+\kappa)\Delta^+ u_j\right] \\ \leq u_{j-1} + \frac{r_{j-1}}{4}\left[(1-\kappa)\Delta^- u_{j-1} + (1+\kappa)\Delta^+ u_{j-1}\right] \end{aligned}$$

we have also, using (3.17)

$$u_j + \frac{r_j}{4}\left[(1-\kappa)\Delta^- u_j + (1+\kappa)\Delta^+ u_j\right] \in I_{j-1} \tag{3.23}$$

From (3.20) and (3.21), and the negation of (*)

$$\begin{aligned} 0 \leq u_{j-1} + \frac{r_{j-1}}{4}\left[(1-\kappa)\Delta^- u_{j-1} + (1+\kappa)\Delta^+ u_{j-1}\right] \\ - \left(u_j + \frac{r_j}{4}\left[(1-\kappa)\Delta^- u_j + (1+\kappa)\Delta^+ u_j\right]\right) \leq \frac{1}{2\nu_{j-1}}(u_j - u_{j-1}) \end{aligned} \tag{3.24}$$

consequently

$$\begin{aligned} 0 \geq & \Phi\left(u_j + \frac{r_j}{4}\left[(1-\kappa)\Delta^- u_j + (1+\kappa)\Delta^+ u_j\right]\ ,\ v_j\right) \\ & - \Phi\left(u_{j-1} + \frac{r_{j-1}}{4}\left[(1-\kappa)\Delta^- u_{j-1} + (1+\kappa)\Delta^+ u_{j-1}\right]\ ,\ v_j\right) \\ \geq & -\frac{a_{j-1}}{2\nu_{j-1}}\Delta^- u_j \end{aligned}$$

and using (3.8),

$$D_{j-\frac{1}{2}} \geq 0$$

If $\Delta^- u_j < 0$, the proof is absolutely similar , obtained by changing the sign of all the preceding inequalities.

($\Diamond$)

Another condition is usually imposed to the extrapolation: one wants the forward and backward discontinuities to be treated in the same way; this induces a symetry condition:

$$r_i \left((1-\kappa)\Delta_i^- + (1+\kappa)\Delta_i^+\right) = l_i \left((1+\kappa)\Delta_i^- + (1-\kappa)\Delta_i^+\right)$$

i.e.

$$\frac{r_i}{l_i} = \frac{1+\kappa+(1-\kappa)\delta_i}{(1-\kappa)+(1+\kappa)\delta_i} \tag{3.25}$$

which must be verified by the limiters for values of δ corresponding to discontinuities, i.e. δ close to 0, or δ very big.

Equations (3.16 - 3.19) plus condition (3.25) give an explicit criteria to select limiters among the numerous ones proposed by different authors (see [28] for a review), or to derive new ones, maybe more compressive in the viscous case.

The most currently used limiters are

- for the fully upwind scheme (κ=-1)

. the "Superbe limiter" due to Roe [21].

$$r(\delta_i) = \text{Max}\{0, \min(2\delta_i, 1), \min(\delta_i, 2)\} \tag{3.26a}$$

$$l(\delta_i) = \text{Max}\{0, \min(2, \delta_i), \min(1, 2\delta_i)\} \tag{3.26b}$$

. which is a particular case of the "ϕ limiters"

$$r(\delta_i) = \text{Max}\{0, \min(\phi\delta_i, 1), \min(\delta_i, \phi)\} \tag{3.27a}$$

$$l(\delta_i) = \text{Max}\{0, \min(\phi, \delta_i), \min(1, \phi\delta_i)\} \tag{3.27b}$$

$$1 \leq \phi \leq 2$$

$\phi = 1$ is the min mod limiter.

. The Van Leer limiter [32]

$$r(\delta_i) = \frac{2\delta_i}{1+\delta_i} \tag{3.28a}$$

$$l(\delta_i) = \frac{2}{1+\delta_i} \tag{3.28b}$$

- for Fromm's scheme (κ=0)

. the Van Albada limiter [29]

$$r(\delta_i) = l(\delta_i) = \frac{2\delta_i}{1+\delta_i^2} \tag{3.29}$$

If we suppose the unlimited scheme to be second order (resp. third order), we must have to keep the second order except at critical points,

$$r(x) = 1 + 0(|x-1|) \tag{3.30a}$$

$$l(x) = 1 + 0(|x-1|) \tag{3.30b}$$

resp.

$$r(x) = 1 + 0(|x-1|^2) \tag{3.31a}$$

$$l(x) = 1 + 0(|x-1|^2) \tag{3.31b}$$

It is easily seen that the preceding limiters all verify the hypothesis of theorem 2, whatever the value of ν, so that they all are unnecessarily diffusive in the viscous case.

Now that we have found the constraints that the slope limiters must verify for the scheme to the T.V.D., we will investigate the influence of κ.

It is clear that the "numerical diffusion" increases when the slope limiters decrease; but κ also has an influence.

Our study will be based on truncature error, and comparison with exact solution, so we will use a scalar steady convection diffusion equation:

$$a u_{,x} - \epsilon u_{,xx} = 0 \tag{3.32a}$$

$$u(0) = 0 \tag{3.32b}$$

$$u(1) = 1 \tag{3.32c}$$

$$a > 0, \epsilon > 0$$

In the unlimited case, equation (3.2) is

$$\begin{aligned} &\frac{a}{h}\left[\frac{1+\kappa}{4}(u_{i+1}-u_i)+\frac{1-2\kappa}{4}(u_i-u_{i-1})-\frac{1-\kappa}{4}(u_{i-1}-u_{i-2})\right] \\ &-\frac{\epsilon}{h^2}(u_{i+1}-2u_i+u_{i-1}) \qquad = 0 \end{aligned} \tag{3.33}$$

Assuming $(u_i)_i$ to be the interpolation of a regular function : $u_i = u(x_i)$, (3.33) is equivalent to:

$$a u'_j - \epsilon u''_j + h^2\left(a\frac{3\kappa-1}{12}u'''_j - \frac{\epsilon}{12}u''''_j\right) + 0(h^3) = 0 \tag{3.34}$$

taking the second derivative of (3.32a), we obtain :

$$a u'''_j = \epsilon u''''_j \tag{3.35}$$

so that, from (3.34), we have third order if :

$$\kappa = \frac{2}{3} \tag{3.36}$$

It appears that although the approximation of u''_j is only second order, third order can be obtained in this linear scalar steady case because the errors due to convection and diffusion eliminate each other when $\kappa = 2/3$.

The exact solution of (3.32) is :

$$u(x) = \frac{\exp(ax/\epsilon) - 1}{\exp(a/\epsilon) - 1} \tag{3.37}$$

replacing u_i by $u(x_i)$= u(ih) in (3.33) we obtain that, to have nodally exact results, we must have :

$$\left(\frac{1}{2} + \frac{\kappa - 1}{4}(1 - \exp(-\frac{ah}{\epsilon})\right) - \left(\frac{\epsilon}{ah} - \frac{1}{\exp(ah/\epsilon) - 1}\right) = 0 \tag{3.38}$$

if we denote by ν the Peclet number,

$$\nu = \frac{ah}{2\epsilon} \tag{3.39}$$

(3.28) gives

$$\kappa = 1 - \frac{2(\coth\nu - 1/\nu)}{1 - \exp(-2\nu)} \tag{3.40}$$

where coth is the hyperbolic cotangent. We have

$$\begin{cases} \kappa(\nu) & \longrightarrow & \frac{2}{3} \\ \nu & \longrightarrow & 0 \end{cases} \quad \text{and} \quad \begin{cases} \kappa(\nu) & \longrightarrow & -1 \\ \nu & \longrightarrow & \infty \end{cases}$$

We find again that when the mesh size tends to zero, the highest order approximation is obtained with $\kappa = 2/3$.

From this study, we conclude that in a boundary layer situation like that defined by (3.32), the best result are obtained with κ given by (3.40), or by a cheaper approximation, at least for small values of the Peclet number. (If ν is bigger than say 2 or 3, there is no possibility to calculate the boundary layer anyway).

Similar results were obtained by Hughes and Mallet [11] ; they studied the same equation (3.32) and concluded that only a fraction of the inviscid numerical diffusion had to be applied in the viscous case, depending on the Peclet number, in a way very much alike to (3.40).

We now propose the following schemes for the nonlinear equation (3.1):

.We use (3.2) where κ is calculated from (3.40), at least for small values of ν (big values of ν will yield $\kappa \approx$ -1, so we can limit the lower value of κ to 0, or even to 1/3) ; in (3.40), we use $\nu = f'(u)h/2\epsilon$ where u is the midpoint of the considered interval (i.e. $u_{i+\frac{1}{2}}$ to calculate $\Phi_{i+\frac{1}{2}}$).

.We limit the extrapolation, using the value of κ obtained in the preceding step, and ν calculated by (3.8), and one of the following formulas:

- "extended superbee":

$$r_j(\delta_j) = \begin{cases} \max\left(0, \min\left(1, \dfrac{4s\delta_j}{(1-\kappa)+(1+\kappa)\delta_j}\right)\right) & \text{if } \delta_j \leq 1 \\ \dfrac{[\min\left(((1+\kappa)+(1-\kappa)\delta_i), 4s\right)]}{(1-\kappa)+(1+\kappa)\delta_i} & \text{if } \delta_j \geq 1 \end{cases} \tag{3.41a}$$

$$l_j(\delta_j) = r_j(\delta_j)\frac{1-\kappa+(1+\kappa)\delta j}{1+\kappa+(1-\kappa)\delta j} \tag{3.41b}$$

$$\text{where} \quad s = \inf\left(k, 1+\frac{1}{2\nu_j}\right) \tag{3.42}$$

The parameter k defines ν_j ; usually k = 1 to avoid a too complicated evaluation of ν_j. This is the most compressive limiter that will match the TVD conditions, it has the disadvantage that it is not equal to 1 in a neighborhood or $\delta_i = 1$, impeaching third order accuracy.

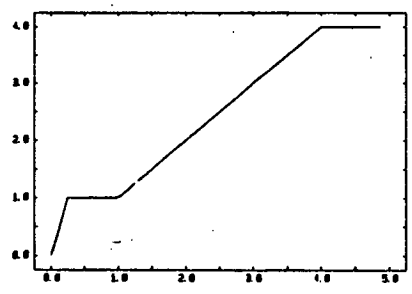

Fig.6a

extended superbee function of δ

$\kappa = -1, \nu = 0.5$

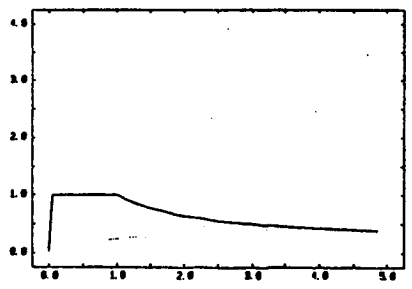

Fig.6b

extended superbee function of δ

$\kappa = \dfrac{2}{3}, \nu = 0.5$

It does verify the symmetry condition (3.25) .

- "third order superbee"

$$r_j(\delta_j) = \begin{cases} \max\left(0, \min\left(1, \dfrac{4s\delta_j}{(1-\kappa)+(1+\kappa)\delta_j}\right)\right) & \text{if } \delta_j \leq 1 \\ 1 \quad \text{if } 1 \leq \delta_j \leq \dfrac{4s-(1-\kappa)}{1+\kappa} & \\ \dfrac{4s}{(1-\kappa)+(1+\kappa)\delta_i} \quad \text{if } \delta_j \geq \dfrac{4s-(1-\kappa)}{1+\kappa} & \end{cases} \tag{3.43.a}$$

$$l_j(\delta_j) = \begin{cases} 1 & \text{if } 1 \geq \delta_j \geq \dfrac{1+\kappa}{4s-(1-\kappa)} \\ r_j(\delta_j)\dfrac{1-\kappa+(1+\kappa)\delta j}{1+\kappa+(1-\kappa)\delta j} & \text{if not} \end{cases} \tag{3.43.b}$$

where s is given by (3.42)

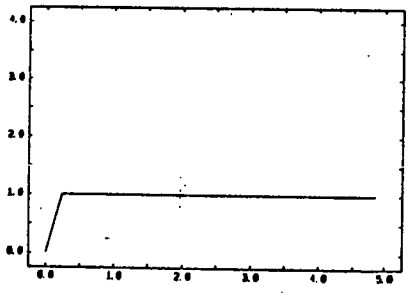

Fig.7a

3rd order extended superbee function of δ

$\kappa = -1, \nu = 0.5$

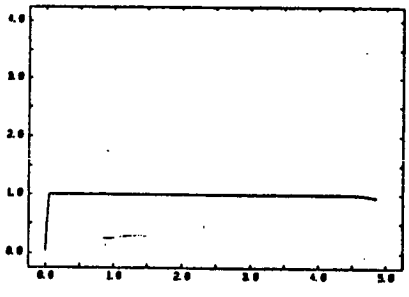

Fig.7b

3rd order extended superbee function of δ

$\kappa = \dfrac{2}{3}, \nu = 0.5$

This limiter preserves third order, but doesn't verify the symmetry condition (3.23) for δ_j close to 1.

Just as the superbee limiter, the ϕ limiters can be extended to in "extended ϕ limiter" and "extended third order ϕ limiter". $\phi = 2$ gives back the superbee. ϕ limiters with ϕ just under 2 are useful for systems, as we will see; ϕ is then a kind of security factor.

-"κ limiter"

It depends on the viscosity through the value of κ only. It is an average of Van Leer's and Van Albada's limiters, derived to be more compressive for high values of κ than for low ones.

$$r_j(\delta_j) = \begin{cases} 0 & \text{if } \delta_j \leq 0 \\ \max\left(\dfrac{4\delta_j}{(1-\kappa)+4\delta_j+(1+\kappa)\delta_j^2}, \dfrac{4\delta_j}{(1-\kappa)(1+\delta_j)+(1+\kappa)(1+\delta_j^2)} \right) & \text{if not} \end{cases} \qquad (3.44.a)$$

$$l_j(\delta_j) = \frac{(1-\kappa)\delta_j + 1 + \kappa}{1-\kappa+(1+\kappa)\delta_j}\, r_j(\delta_j) \qquad (3.45b)$$

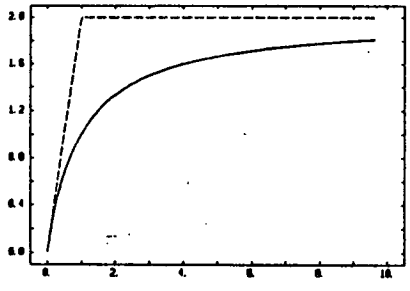

Fig.8a

κlimiter function of δ

$\kappa = -1, \nu = 0.5$

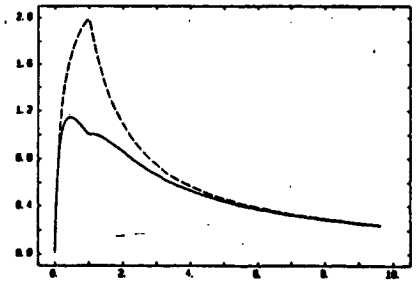

Fig.8b

κlimiter function of δ

$\kappa = \frac{2}{3}, \nu = 0.5$

This limiter is less compressive than the two preceeding one, but has smoother variations.

IV. EXTENSION TO THE MULTIDIMENSIONAL NAVIER STOKES SYSTEM

The usual way to reduce a two or three dimensional system to a scalar conservation law is:

- projection of the equation on the direction normal to the boundary of the cell, through the finite volume formulation. One obtains then a one dimensional system.
- diagonalization of this system.

We will restrict ourselves to the two dimensional case for simplicity but the generalization to 3D is straightforward.

The Navier-Stokes system, in matrix form, reads :

$$\frac{\partial W}{\partial t} + \nabla.(F(W)) - \nabla.(D(W).\nabla W) = 0 \tag{4.1}$$

$$D(W).\nabla W = \frac{1}{Re} N(W)$$

D(W) is an 8 x 8 (15 x 15 in 3D) matrix. The finite volume formulation, as explained in section II, is based on:

$$\frac{d}{dt}\left(\int_{Ci} W\right) + \sum_{j \in K(i)} \left(\int_{\partial S_{ij}} \widetilde{F}(W).\nu_i - \int_{\partial S_{ij}} \nu_i.D(W).\nabla W \right) = 0 \tag{4.2}$$

in which we have dropped the boundary term, and where $\widetilde{F}$ is some approximation of F, ν_i the outward unit vector to ∂C_i, $\nu_i = (\nu_{ix}, \nu_{iy})$;

$$\nabla W = \begin{pmatrix} W,x \\ W,y \end{pmatrix} \tag{4.3}$$

$$\nu_i.D(W).\nabla W = (\nu_{ix} D_1(W) + \nu_{iy} D_2(W)).\nabla W \tag{4.4}$$

$\nu_{ix}\ D_1 + \nu_{iy}\ D_2$ is a (4 x 8) matrix .

One way to apply one dimensional theory is to consider the one dimensional system obtained by two local projections on the normal direction:

$$\frac{\partial W}{\partial t} + A_n(W)\frac{\partial W}{\partial n} - \frac{\partial}{\partial n}\left(D_n(W)\frac{\partial W}{\partial n}\right) = 0 \tag{4.5}$$

$$\text{where} \qquad A_n = \frac{\partial(F(W).n)}{\partial W} \tag{4.6}$$

$$\text{and} \qquad D_n(W) = \nu_x^2 D_{11}(W) + \nu_x\nu_y(D_{12}(W) + D_{21}(W)) + \nu_y^2 D_{22}(W) \tag{4.7}$$

$$D(W) \quad = \quad \begin{pmatrix} D_1(W) \\ D_2(W) \end{pmatrix} \quad = \quad \begin{pmatrix} D_{11}(W) & D_{12}(W) \\ D_{21}(W) & D_{22}(W) \end{pmatrix} \tag{4.8}$$

Then, it is easy to see that there is an invertible matrix P, which diagonalizes the convection operator, and symmetrizes the diffusion operator.

$$P^{-1}A_nP = \text{diag}\ (u.\nu, u.\nu, u.\nu + c, u.\nu - c) \tag{4.9}$$

$$P^{-1}D_nP = \frac{1}{\rho Re}\begin{pmatrix} \frac{1}{Pr} & 0 & -\sqrt{\frac{\gamma-1}{2}}\frac{1}{Pr} & -\sqrt{\frac{\gamma-1}{2}}\frac{1}{Pr} \\ 0 & 1 & 0 & 0 \\ -\sqrt{\frac{\gamma-1}{2}}\frac{1}{Pr} & 0 & \frac{2}{3} + \frac{\gamma-1}{2Pr} & -\frac{2}{3} + \frac{\gamma-1}{2Pr} \\ -\sqrt{\frac{\gamma-1}{2}}\frac{1}{Pr} & 0 & -\frac{2}{3} + \frac{\gamma-1}{2Pr} & \frac{2}{3} + \frac{\gamma-1}{2Pr} \end{pmatrix} \tag{4.10}$$

$$P^{-1} = \begin{pmatrix} \sqrt{\frac{\gamma-1}{2}} & 0 & \frac{1}{2} & \frac{1}{2} \\ \sqrt{\frac{\gamma-1}{2}}u & \sqrt{\frac{\gamma-1}{2}}\nu_y & \frac{u+C\nu_x}{2} & \frac{u-C\nu_x}{2} \\ \sqrt{\frac{\gamma-1}{2}}u & -\sqrt{\frac{\gamma-1}{2}}\nu_x & \frac{v+C\nu_y}{2} & \frac{v-C\nu_y}{2} \\ \sqrt{\frac{\gamma-1}{8}}(u^2+v^2) & \sqrt{\frac{\gamma-1}{2}}(\nu_y u - \nu_x v) & \frac{H+(\nu_x u+\nu_y v)C}{2} & \frac{H-(\nu_x u+\nu_y v)C}{2} \end{pmatrix} \tag{4.11}$$

$$H = \frac{E+P}{\rho}$$

$$P = \begin{pmatrix} \sqrt{\frac{2}{\gamma-1}} - \sqrt{\frac{\gamma-1}{2}}\frac{u^2+v^2}{C^2} & \sqrt{\frac{\gamma-1}{2}}\frac{u}{C^2} & \sqrt{\frac{\gamma-1}{2}}\frac{v}{C^2} & -\sqrt{\frac{\gamma-1}{2}}\frac{1}{C^2} \\ \sqrt{\frac{2}{\gamma-1}}(\nu_x v - \nu_y u) & \sqrt{\frac{2}{\gamma-1}}\nu_y & -\sqrt{\frac{2}{\gamma-1}}\nu_x & 0 \\ -\frac{\nu_x u+\nu_y v}{C} + \frac{\gamma-1}{C^2}\left(\frac{u^2+v^2}{2}\right) & \frac{\nu_x-(\gamma-1)u/C}{C} & \frac{\nu_y-(\gamma-1)v/C}{C} & \frac{\gamma-1}{C^2} \\ \frac{\nu_x u+\nu_y v}{C} + \frac{\gamma-1}{C^2}\left(\frac{u^2+v^2}{2}\right) & -\frac{\nu_x+\gamma-1u/C}{C} & -\frac{\nu_y+\gamma-1v/C}{C} & \frac{\gamma-1}{C^2} \end{pmatrix} \tag{4.12}$$

The eigenvalues and eigenvectors of $P^{-1}D_nP$ are:

$$\lambda_1 = 0 \qquad r_1 = \begin{pmatrix} \sqrt{\frac{\gamma-1}{\gamma}} \\ 0 \\ \frac{1}{\sqrt{2\gamma}} \\ \frac{1}{\sqrt{2\gamma}} \end{pmatrix} \tag{4.13a}$$

$$\lambda_2 = \frac{1}{\rho Re} \qquad r_2 = \begin{pmatrix} 0 \\ 1 \\ 0 \\ 0 \end{pmatrix} \tag{4.13b}$$

$$\lambda_3 = \frac{4}{3\rho Re} \qquad r_3 = \begin{pmatrix} 0 \\ 0 \\ \frac{1}{\sqrt{2}} \\ \frac{1}{\sqrt{2}} \end{pmatrix} \tag{4.13c}$$

$$\lambda_4 = \frac{\gamma}{\rho Re Pr} \qquad r_4 = \begin{pmatrix} \frac{1}{\sqrt{\gamma}} \\ 0 \\ -\sqrt{\frac{\gamma-1}{2\gamma}} \\ -\sqrt{\frac{\gamma-1}{2\gamma}} \end{pmatrix} \tag{4.13d}$$

In the steady case, it is even possible to diagonalize $|A_n|^{-1} D_n$, the eigenvalues are :

$$0, \quad \frac{1}{\rho Re|u|}, \quad \frac{1}{\rho Re}\frac{a+b \pm \sqrt{(a-b)^2+c^2}}{2}$$

with $a = \frac{2Pr}{3}\left(\frac{1}{|u+c|}+\frac{1}{|u-c|}\right)$, $b = \frac{1}{|u|}+\frac{\gamma-1}{2}\left(\frac{1}{|u+c|}+\frac{1}{|u-c|}\right)$,

$$c = \frac{2Pr}{3}\left(\frac{1}{|u+c|}+\frac{1}{|u-c|}\right)$$

To choose the extrapolation parameter and slope limiter locally, it is possible to use the results of III applied to each of the characteristic component Vi of the steady linearized equation:

$$|A_n|^{-1} A_n U_{,x} - |A_n|^{-1} D_n U_{,xx} = 0 \tag{4.14}$$

$$\Longleftrightarrow \begin{cases} a_i Vi_x - \epsilon_i Vi_{xx} = 0 \\ i = 1,4 \end{cases} \tag{4.15}$$

where a_i is an eigenvalue of $|A_n|^{-1} A_n$,$(a_i = \pm 1)$, and ϵ_i is the corresponding eigenvalue of $|A_n|^{-1} D_n$.

However, as the diffusion matrix D is not block-diagonal, i.e. as cross derivatives appear in the diffusion term, this analysis breaks down when these cross derivatives are of importance . It is also our numerical experience that this manner of extending one dimensional results to multidimensional equations is not satisfactory because the diffusion is under estimated.

This is why, following, among others, Roe [22], we use an alternate projection, in which the physical viscosity is estimated as the ratio of the diffusion flux to a reference flux: for each characteristic direction, for each vertex S_i, each j $\in \kappa(i)$, we compute, for the four characteristic fields,

$$a_k = \begin{cases} \max\left(|(u.\nu_i)(S_i)|, |(u.\nu_i)(S_j)|\right) & \text{for } k = 1,2 \\ \max\left(|(u.\nu_i)(S_i) + C(S_i)|, |(u.\nu_i)(S_j) + C(S_j)|\right) & \text{for } k = 3 \\ \max\left(|(u.\nu_i)(S_i) - C(S_i)|, |(u.\nu_i)(S_j) - C(S_j)|\right) & \text{for } k = 4 \end{cases} \tag{4.16}$$

and

$$\epsilon_k = \frac{1}{Re} \frac{\left| l_k \left(\frac{W_i+W_j}{2}\right) . N \left(\frac{W_i+W_j}{2}\right) . \nu_i \right|}{\left| l_k \left(\frac{W_i+W_j}{2}\right) . \frac{W_i - W_j}{\|\overrightarrow{S_i S_j}\|} \right|} \tag{4.17}$$

where l_k is the corresponding left eigenvector.

We then calculate the Peclet number :

$$\nu_k = \frac{a_k \|\overrightarrow{S_i S_j}\|}{2\epsilon_k} \tag{4.18}$$

and the corresponding κ_k from (3.40), the corresponding limiters L_{ij}^k (resp. L_{ji}^k) from one of the formulas (3.41), (3.43) or (3.45), (resp. (3.42), (3.44) or (3.46)) in which (see Fig 3):

$$\delta_i^k = \frac{l_k \left(\frac{W_i+W_j}{2}\right) . \nabla W_{ij} . \overrightarrow{S_i S_j}}{l_k \left(\frac{W_i+W_j}{2}\right) . \nabla W|_{T_{ij}} . \overrightarrow{S_i S_j}} \tag{4.19}$$

$$\delta_j^k = \frac{l_k \left(\frac{W_i+W_j}{2}\right) . \nabla W|_{T_{ji}} . \overrightarrow{S_i S_j}}{l_k \left(\frac{W_i+W_j}{2}\right) . \nabla W_{ij} . \overrightarrow{S_i S_j}} \tag{4.20}$$

We then carry out an extrapolation similar to (2.28) :

$$\begin{cases} W_{ij} = W_i + \Pi_{ij} E_{ij}^1 \Pi_{ij}^{-1} \left(\nabla W_{ij} . \overrightarrow{S_i S_j}\right) + \Pi_{ij} E_{ij}^2 \Pi_{ij}^{-1} \left(\nabla W|_{T_{ji}} . \overrightarrow{S_i S_j}\right) \\ W_{ji} = W_j - \Pi_{ij} E_{ji}^1 \Pi_{ij}^{-1} \left(\nabla W_{ji} . \overrightarrow{S_i S_j}\right) - \Pi_{ij} E_{ji}^2 \Pi_{ij}^{-1} \left(\nabla W|_{T_{ji}} . \overrightarrow{S_i S_j}\right) \end{cases} \tag{4.21}$$

with

$$E_{ij}^1 = diag\left(L_{c_{ij}}^k \frac{1-\kappa_k}{4} \quad , \quad k=1,...,4\right) \tag{4.22a}$$

$$E_{ij}^2 = diag\left(L_{c_{ij}}^k \frac{1+\kappa_k}{4} \quad , \quad k=1,...,4\right) \tag{4.22b}$$

$$E_{ji}^1 = diag\left(L_{c_{ji}}^k \frac{1-\kappa_k}{4} \quad , \quad k=1,...,4\right) \tag{4.22c}$$

$$E_{ji}^2 = diag\left(L_{c_{ji}}^k \frac{1+\kappa_k}{4} \quad , \quad k=1,...,4\right) \tag{4.22d}$$

Both the extrapolation parameter κ and the slope limiters are defined locally, and for each characteristic field ; the extra computational cost is reasonable, since both the eigenvectors l_k and the diffusion flux $\nu.(D(W).\nabla W)$ are already calculated. Formula (3.40) can be replaced by a cheaper function, to avoid the computation of exponentials.

V. RESOLUTION ALGORITHM

The spatial discretization procedures described in the previous sections lead to semi-discretized formulations which has to be integrated until they reach a steady state.

An explicit version can be derived by using a diagonal mass-lumped matrix:

$$D = \text{diag}\left[\frac{aera(S_i)}{\Delta t_i}\right]$$

in the time derivative term integration.

The time step Δt_i can be set equal to constant for first-order accurate time integration, or taken equal to the value matching a local stability condition for steady state computation.

The resulting scheme is given by:

$$\begin{aligned} D\left(W_h^{n+1} - W_h^n\right)_i = &- \sum_{j\in K(i)} H_{ij}^{(2)}(W_h^n) - \int_{\partial S_{ij}\cap\Gamma} F(W_h^n) n d\sigma \\ &+ \frac{1}{Re}\sum_{j\in K(i)} \int_{\partial S_{ij}} N(W_h^n).\nu_i d\sigma + \frac{1}{Re}\int_{\partial S_{ij}\cap\Gamma} N(W_h^n) n d\sigma \end{aligned} \tag{5.1}$$

We can also use a multistage time stepping scheme ; the stability condition would be less restrictive. An interesting study on the use of such time integrators combined with upwind approximations can be found in [MHL] in the inviscid case.

All these explicit schemes are easy to implement, but generally give slow convergence to steady-state because the associated stability conditions lead to the use of small time-steps.

In order to get rid of these too restrictive conditions, one attempts to design implicit algorithms. In that direction, a linearized procedure for each term is applied on equation (5.1), once we have replaced W_h^n by W_h^{n+1}. Firstly, the convection term is treated as follows:

$$H_{ij}^{(2)}(W_h^{n+1})$$

is linearized as

$$H_{ij}^{(2)}(W_h^n) + J_{ij}\delta W_h^n$$

with

$$J_{ij} = \frac{dH_{ij}^{(2)}}{dW}$$

and

$$\delta W_h^n = W_h^{n+1} - W_h^n \tag{5.2}$$

The computation of such a Jacobian matrix considering the complexity of the term $H_{ij}^{(2)}$ would be too complicated and too costly. So, three simplifications in this evaluation are made :

- The matrix J_{ij} is replaced by $dH_{ij}^{(1)}/dW$ relying on the first order accurate approximation.

- We do not linearize the Osher approximate Riemann solver but we use the simpler Steger-Warming flux splitting. One can find in [20] a possible justification of this point.

- We only retain in the evaluation of the Jacobian matrix the "homogeneous" part of it.

It means that the approximate Jacobian is given by

$$J_{ij} = P_{ij}^{+}(W_i^n)\delta W_i^n + P_{ij}^{-}(W_j^n)\delta W_j^n \tag{5.3}$$

The viscous internal term is linearized in a straightforward manner as

$$\frac{1}{Re}\sum_{j\in K(i)}\left[\int_{\partial S_{ij}} N(W_h^n).\nu_i d\sigma + \int_{\partial S_{ij}} \frac{dN}{dW}(W_h^n).\nu_i \delta W_h d\sigma\right] \tag{5.4}$$

The numerical integration is performed as described in the previous sections. Details on the computations of the matrix $dN/dW(W_h^n).\nu_i$ are given in [23].

The convective (resp. viscous) boundary integral is linearized similarly as the convection internal (resp. viscous) term.

For degrees of freedom belonging to the wall boundary, as Dirichlet boundary conditions are imposed, the matrix is loaded in order that the increment δW_h^n satisfies the linearized Dirichlet boundary conditions.

Once this linearization procedure is done, the implicit formulation is given by:

$$\begin{aligned} M(W_h^n)\left(W_h^{n+1} - W_h^n\right)_i = &- \sum_{j\in K(i)} H_{ij}^{(2)}(W_h^n) - \int_{\partial S_{ij}\cap\Gamma} F(W_h^n) n d\sigma \\ &+ \frac{1}{Re}\sum_{j\in K(i)}\int_{\partial S_{ij}} N(W_h^n).\nu_i d\sigma + \frac{1}{Re}\int_{\partial S_{ij}\cap\Gamma} F(W_h^n) n d\sigma \end{aligned} \tag{5.5}$$

where $M(W_h^n)$ is the sum of all the constructed Jacobian matrices.

This matrix is a sparse block 4 x 4 matrix (5 x 5 in 3D) without any simple structure.

In the inviscid case, nodewise collective relaxation iterative methods to solve the system (5.5) have proved to be very efficient in this unstructured situation [26]. We use the same technique which can be Gauss-Seidel relaxation or Jacobi for vectorization purposes if any.

Larger time steps then for explicit methods can be used in this implicit approach. At the end, the effficiency of the method is verified, despite that it is only a quasi-Newton procedure because of the drastic simplifications made in the evaluation of the Jacobian.

VI. NUMERICAL RESULTS

We first compared the results of the unlimited scheme ($r_j = l_j = 1$) for different values of κ. A transonic flow at a mach number of $M_\infty = 0.85$ and a constant Reynolds number of 500 was computed on an undermeshed grid (3114 nodes), for κ = -1 and $\kappa = 2/3$. On figure 9, the iso-Mach lines are compared. The fully upwind scheme ($\kappa = -1$, 9b) yields more numerical viscosity as can be seen in the wake, while the third order scheme ($\kappa = 2/3$, 9a) allows spurious oscillations behind the schock, although very weak, but gives a better result in the wake and, though less obvious, in the boundary layer. This confirms our statement that different values of κ are needed in different zones, depending on the local Peclet number.

The history of convergence in the case of $\kappa = 2/3$ is presented on fig. 10 ; (10 a) shows the logarithm of the residual versus the number of time steps for the explicit scheme, (10 b) is the same for the implicit scheme, (10 c) is a comparison of the two schemes in terms of CPU time on CRAY II. Machine-precision convergence is achieved in 150 time steps or 120 seconds by the implicit scheme, while the explicit scheme takes 1200 time steps or 240 seconds to reach a residual superior to 0.001. For a steady calculation, the use of the implicit scheme divides the needed CPU time by more than 10, although the expected Newton-like quadratic convergence is not achieved.

The viscosity dependent κ,together with the unlimited scheme was used to compute the same flow on an adapted mesh, still rather coarse (fig. 11, 2970 nodes), and on a thinner mesh (fig. 12, 5712 nodes). The mesh, the iso-mach lines and the pressure coefficients on the body are compared. It can be seen that a good solution is obtained on the smaller grid, although quite coarse.

To compare the limiters, a hypersonic flow over a flat plate was computed. The mach number is $M_\infty = 10$, the Reynolds number $Re/m = 5.10^5$, the length of the plate is 2, the temperature at the inflow is 83,5K the temperature at the wall is 525 K; Sutherland's law is used. A first computation was made with the κ limiter, and the viscosity dependant κ. The mesh (fig. 13 a, partial view), speed vectors (fig. 13 b), pressure coefficient (fig. 13 c) and skin friction coefficient compared with laminar boundary layer theory results (fig. 13 d) are presented.

There are about 15 nodes in the boundary layer. The shock at x = 0 is captured ; no oscillation is seen. The agreement with theory is excellent; the same flow was computed with the Van Albada limiter and $\kappa = 1/3$, giving extremely similar results (not shown), so we consider this result as a reference, and use a coarser grid. The same flow is computed on a mesh with 8 nodes in the boundary layer, using $\kappa = 1/3$ and the Van Albada limiter for the non linear fields, and the viscosity dependent κ with the κ-limiter for the contacts. The κ limiter was experimented to be too compressive for using on the nonlinear waves. Figure 14 shows the speed vectors. Figure 15 is a comparison of skin friction obtained on the preceeding grid (full), using $\kappa = 1/3$, Van Albada limiter for the four fields (long broken), using for the contacts the "third order Φ limiter", with $\Phi = 1.6$ and the viscosity dependent κ (short broken), or the κ limiter and viscosity dependant κ (broken doted). Figure 16 shows the skin friction on the second half of the plate, for schemes which all use $\kappa = 1/3$, Van Albada limiter for the nonlinear fields, and the viscosity dependent κ for the contact discontinuities. It is seen that the "extended superbee", or "extended Φ limiters", are too compressive, even

for a contact, but that both the "κ limiter" and "third order extended Φ limiter" with $\Phi \simeq 1.6$ give results in agreement within one or two percents with our reference result, at least on the second half of the plate. This is an improvement over the $\kappa = 1/3$, Van Albada limiter, which gives more than 10 % error.

Another hypersonic computation was performed around an ellipse : the Mach number is $M_\infty = 8$, the Reynolds number is constant and worth $Re_\infty/m = 1000$, the angle of attack is $\alpha = 40^o$. The mesh and iso-Mach lines are shown (fig. 17). There is no overshoot at the shock and with the implicit scheme, the after body flow can be computed without any special treatment ; this cannot be achieved with an explicit code. The mesh was adapted by an automatic local mesh refinment algorithm, due to C. Pouletty [19] and B. Palmerio [18].

An easier calculation was performed to compare the convergence of the explicit and implicit codes : fig. 18 shows the convergence history for a flow around an ellipse at a mach number of 4, for the explicit and implicit scheme.The mesh has 1378 nodes (not shown).It is seen that the implicit scheme allows schock capturing with a courant number C = 100

IV. CONCLUSION

A numerical scheme to solve the compressible Navier-Stokes equations on unstructured meshes, based on a "TVD" finite volume formulation, has been obtained, by extending a method first derived for inviscid gas. We have obtained a condition on the limiters for the scheme to be TVD, taking into account the physical viscosity. Different limiters have been proposed which match this condition, and compared from a numerical point of view. The upwinding also depends on the local amount of physical viscosity. It has been shown that laminar boundary layers can be calculated with our scheme, on a triangular mesh, with less than ten nodes in the boundary layer.

An efficient algorithm has been proposed for the steady case, which allows cheap computation of very stiff problems, as hypersonic flows on ge-

ometries with rear body. Really unsteady flow remain a challenge because of their computational cost.

Aknowledgments :

P.Rostand is supported by DRET contract n_o 03 40 79 01.

The computations where made on the CRAY II of C.C.V.R.

References :

[1] F.Angrand,"Numerical Simulations of Compressible Navier Stokes Flows", GAMM Workshop,M.O.Bristeau,R.Glowinski, J.Periaux,H.Viviand (eds),Friedr. Vieweg und Sohn,1987,p 69-85.

[2] F.Angrand,A.Dervieux,"Some Explicit Triangular Finite Element Schemes for the Euler Equations",International Journal for Numerical Methods in Fluids, vol. 4,749-764 (1984).

[3] F.Angrand,J.Erhel,"Vectorized F.E.M. codes for compressible flows", Proc. of the 6th International Symposium on Finite Element Methods in flow problems,Antibes,Juin 1896.

[4] K.Baba,M.Tabata,"On a Conservative Upwind Finite Element Scheme for Convection Diffusion Equations",RAIRO Numerical Analysis,15 n1,1981.

[5] G.V.Candler,R.W.Mac Cormack, "Hypersonic Flow past 3D Configurations", AIAA 87-0480,Reno,January 12-16,1987.

[6] S.Chakravarthy,"High Resolution Upwind Formulations for the Navier-Stokes Equations",Von Karman Institute Lecture Series 1988-05,March 7-11, 1988.

[7] A.Dervieux,"Steady Euler Simulations using Unstructured Meshes", Von Karman Institute Lecture Series,1983.

[8] B. Engquist and S. Osher, "Stable and entropy satisfying approximations for transonic flow calculations", Math. Comp. V. 34, 1980, pp. 45-75.

[9] B. Engquist and S. Osher,"One sided difference approximations for nonlinear conservation laws", Math. Comp. V. 36, 1981, pp. 321-352.

[10] A. Harten, "High resolution schemes for hyperbolic conservation laws", JCP, Vol. 49, pp. 357-393, 1983.

[11] T.J.R.Hughes,M.Mallet,"A New Finite Element Formulation for Computational Fluid Dynamics:III The Generalized Streamline Operator for Multidimensional Advective-Diffusive Systems", Computer Methods in Applied Mechanics and Engineering,n^o 58,1986,p 305-328.

[12] M.H.Lallemand,"Schemas Decentres Multigrilles pour la Resolution des equations d'Euler en elements finis",Thesis,Universite de Provence,Mars 1986.

[13] R.Lohner,K.Morgan,J.Peraire,O.C.Zenkiewitcz,L.Kong, "Finite Element Methods for Compressible Flows", Proceedings of the conference on Numerical Methods for Fluid Dynamics, Reading, April 1985.

[14] L.Martinelli,A.Jameson, "Validation of a Multigrid Method for the Rrynolds Averaged Equations",AIAA paper 88-0414,Reno 1988.

[15] S. Osher, "Convergence of generalized MUSCL schemes", ICASE-NASA contractor report 172-306, Feb. 1984.

[16] S.Osher,S.Chakravarthy,"Upwind difference schemes for the hyperbolic systems of conservation laws", Mathematics of Computation,April 1982.

[17] S.Osher,S.Chakravarthy,"High resolution schemes and the entropy condition", SIAM J. Num. An. Vol. 21, n^o 5, October 1985.

[18] B.Palmerio,"Self Adaptive F.E.M. Algorithms for the Euler Equations", INRIA report 338,1985.

[19] C.Pouletty,"Generation et Optimisation de Maillages en Elements Finis,Application a la resolution des equations de la mecanique des fluides",These de Docteur Ingenieur,Ecole Centrale,Dec 1985.

[20] M.S.Rai,S.Chakravarthy, "An implicit form of the Osher upwind scheme", AIAA paper 84-0088, Reno 1984.

[21] P.L. Roe, "Some contributions to the modelling of discontinuous flows", Proc. AMS/SIAM Seminar, San Diego, 1988.

[22] P.L. Roe, "Finite volume methods for the compressible Navier-Stokes equations", Proceedings of "Numerical methods on Laminar and Turbulent flow", Montreal, 1987.

[23] P.Rostand,Thesis,Université Paris VI,in preparation.

[24] R. Sanders, "On convergence of monotone finite difference schemes with variable spatial differencing", Math. Comp. 40, (1983), pp. 91-106.

[25] R.Schwane,D.Hanel,"Computation of Viscous Supersonic Flows around Blunt Bodies,7th GAMM Conference on Numerical Methods in Fluid Mechanics,Louvain la Neuve,1987.

[26] B. Stoufflet,L.Fezoui,"A Class of Implicit Upwind Schemes for Euler Simulations with Unstructured Meshes",to appear.

[27] B. Stoufflet,J.Periaux,L.Fezoui,A.Dervieux,"Numerical Simulations of 3-D Hypersonic Euler Flows Around Space Vehicles Using Adapted Finite Elements",AIAA paper 87 0560 Reno 1987.

[28] P.K. Sweby, "High resolution schemes using flux limiters for hyperbolic conservation laws", SIAM J. of Num. An., Vol. 21, n^o 5, October 1984.

[29] G.D. Van Albada, B. Van Leer, W.W. Roberts, Jr. (1982), Astron. Astrop. 108, 1976.

[30] B.Van Leer,J.L.Thomas,P.L.Roe,R.W.Newsome,"A Comparison of Numerical Flux Formulas for the Euler and Navier Stokes Equations",proceedings of the AIAA Honolulu meeting,1987,p 36-41.

[31] B.Van Leer,"Computational Methods for Ideal Compressible Flow",Von Karman Institute for fluid dynamics,lecture series 1983-04,Computational Fluid Dynamics, March 7-11 1983.

[32] B. Van Leer, "Towards the ultimate conservative difference scheme, II. Monotonicity and conservation combined in a second order scheme", JCP, 14 (1974), pp. 361-370.

[33] H.C.Yee,"Upwind and Symetric Shock-Capturing Schemes",NASA TM 89464,May 1987.

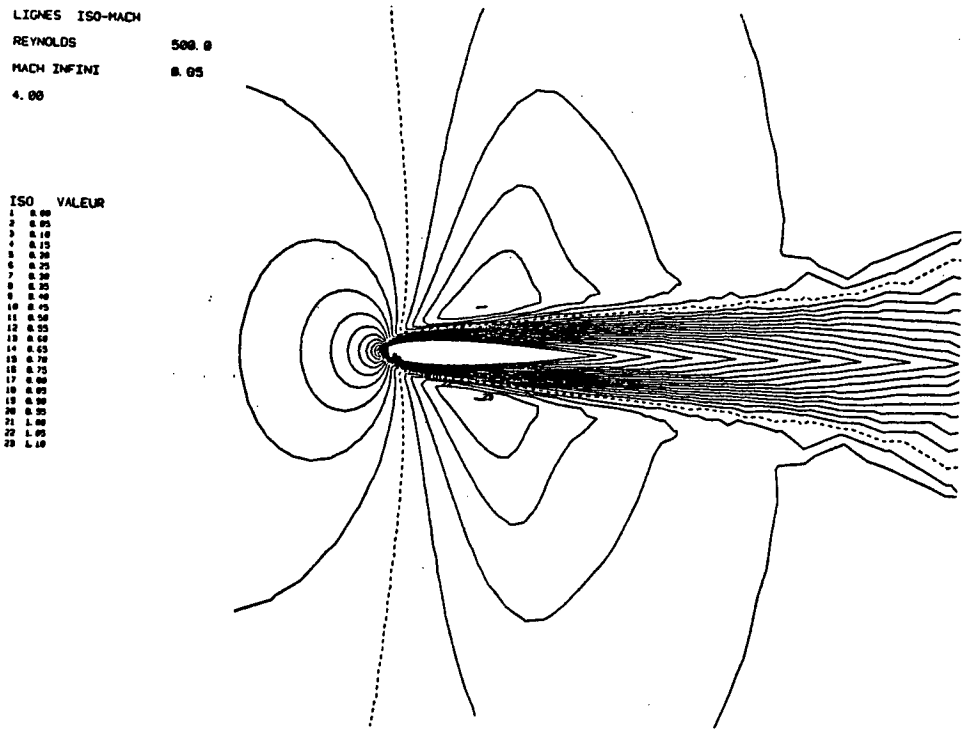

fig. 9a : $\kappa = \frac{2}{3}$

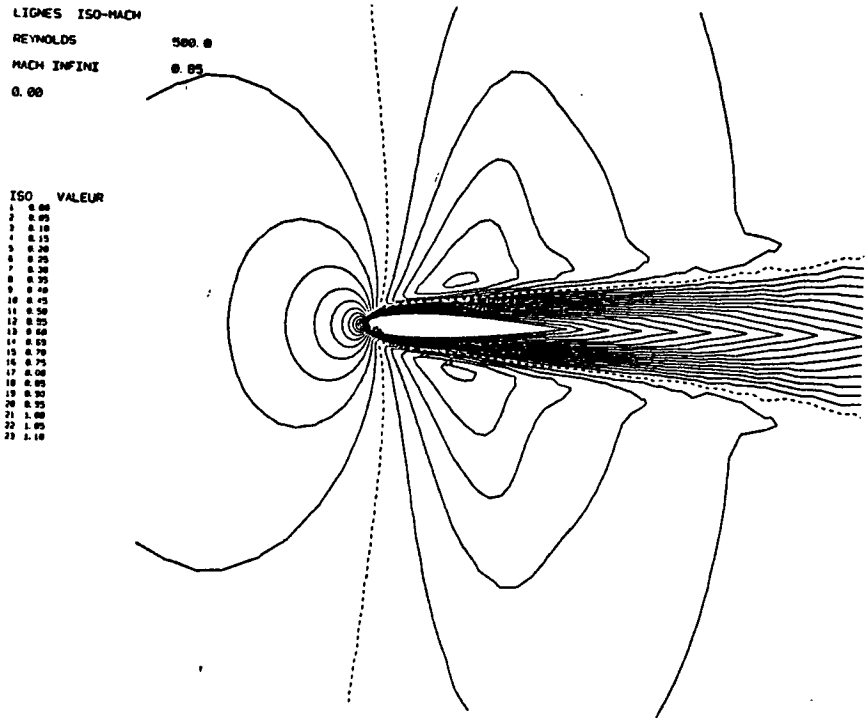

fig. 9b : $\kappa = -1$

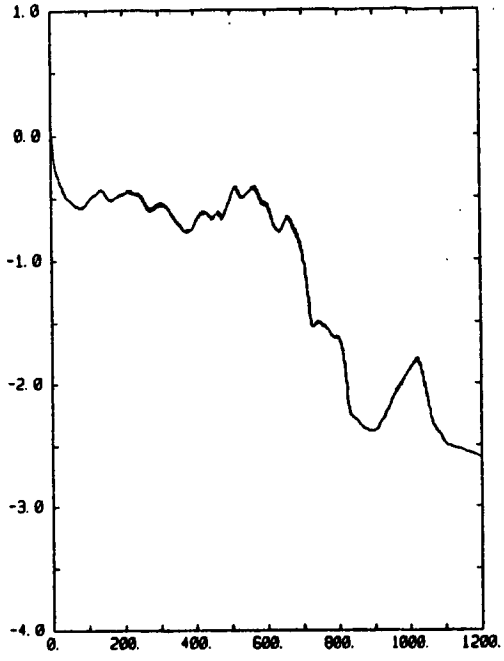

fig. 10a

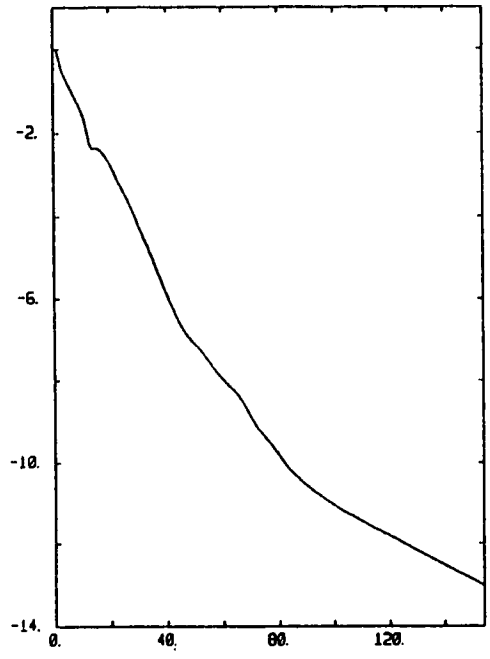

fig. 10b

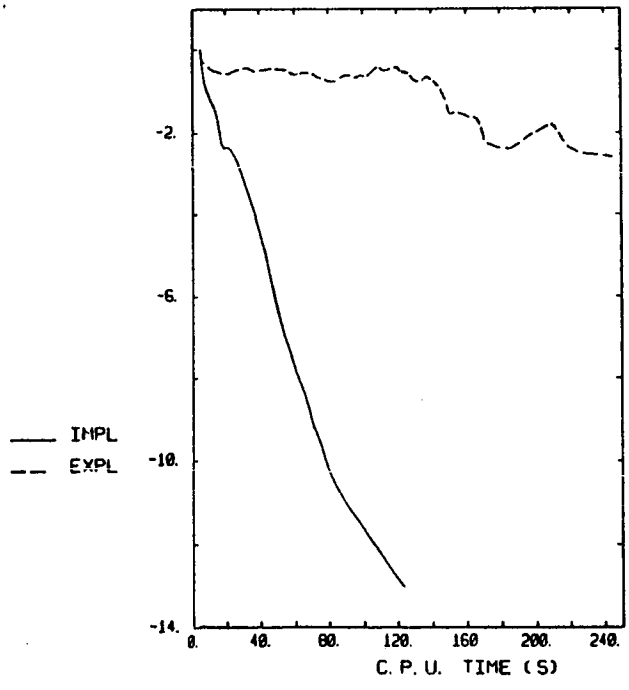

fig. 10c

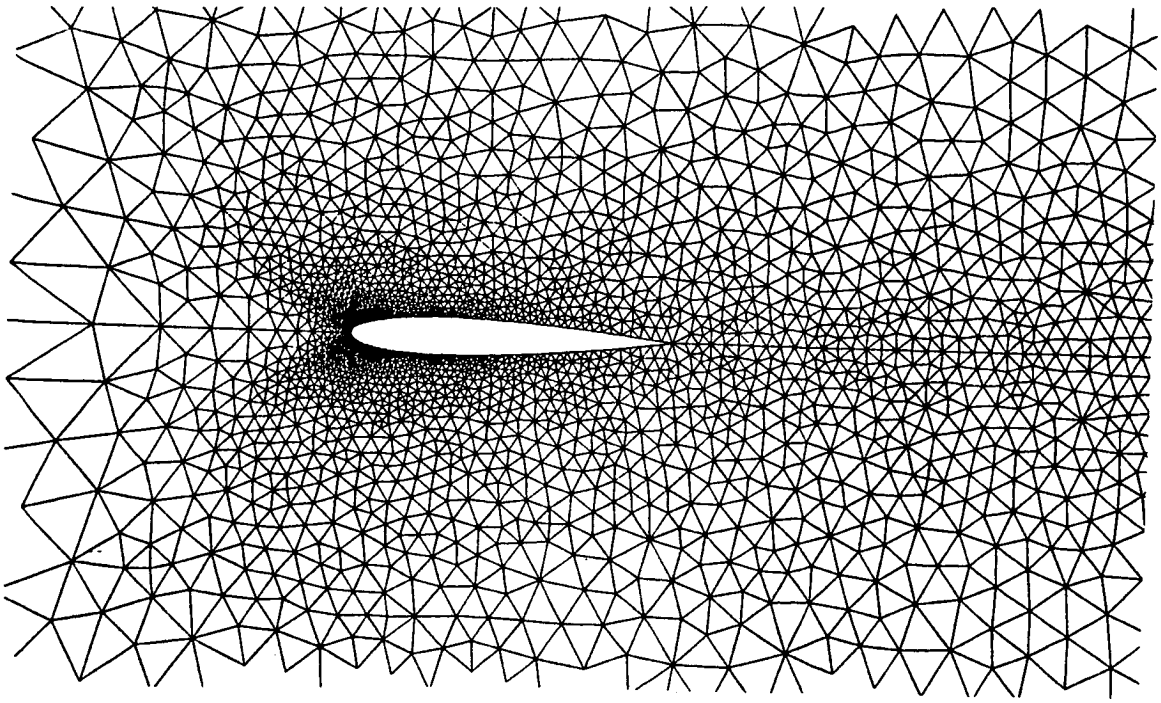

fig. 11a : 2970 Nodes, 5764 Elements (partial view)

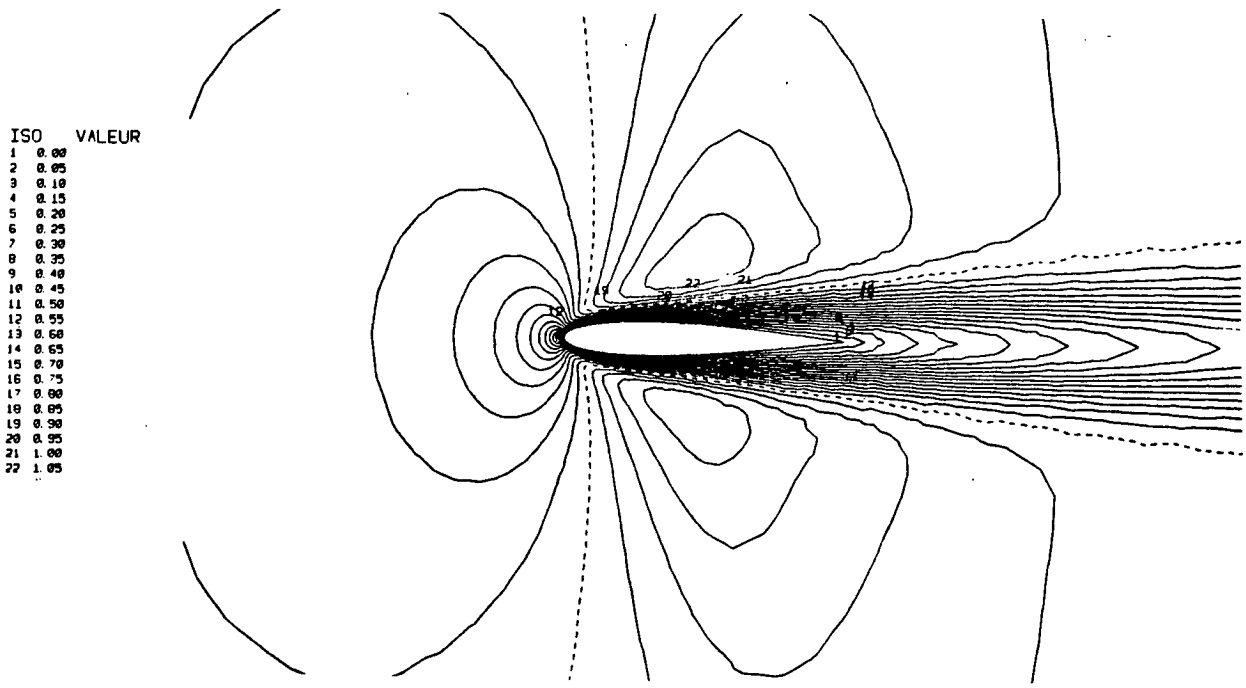

fig. 11b : iso Mach lines

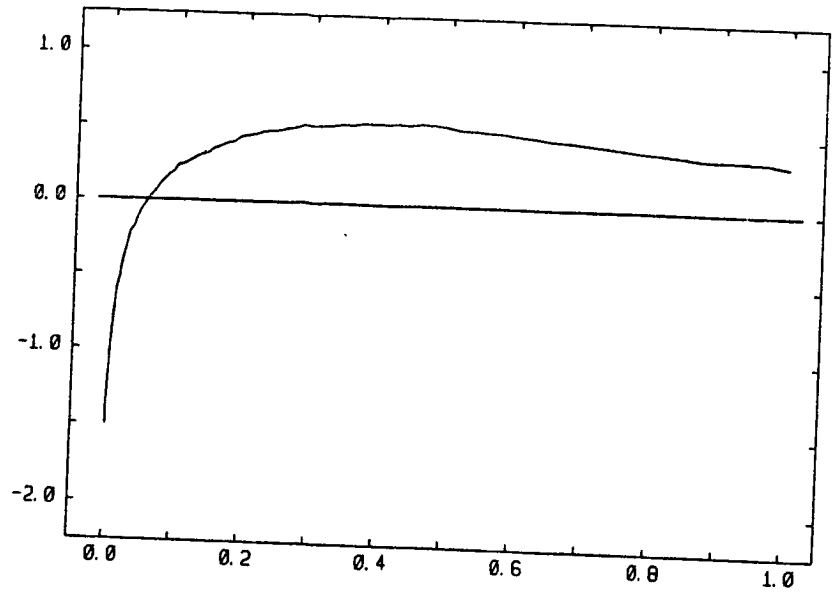

fig. 11c : pressure coefficient

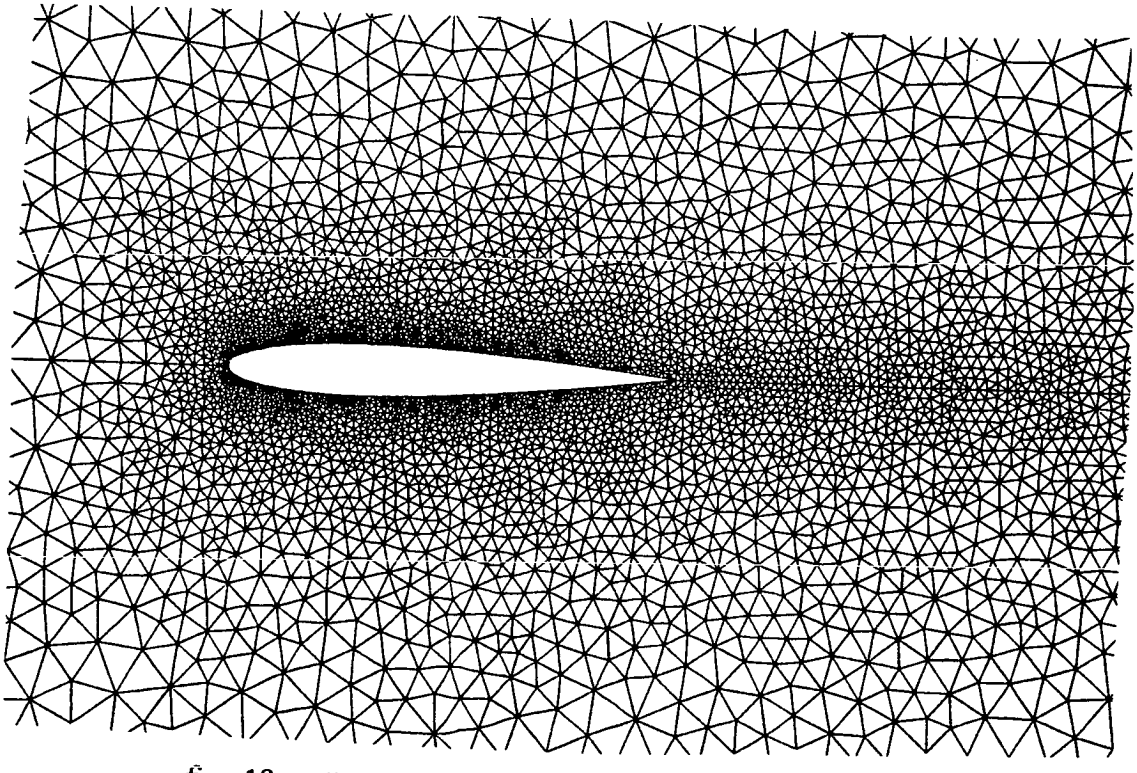

fig. 12a : 5712 Nodes, 11184 Elements (partial view)

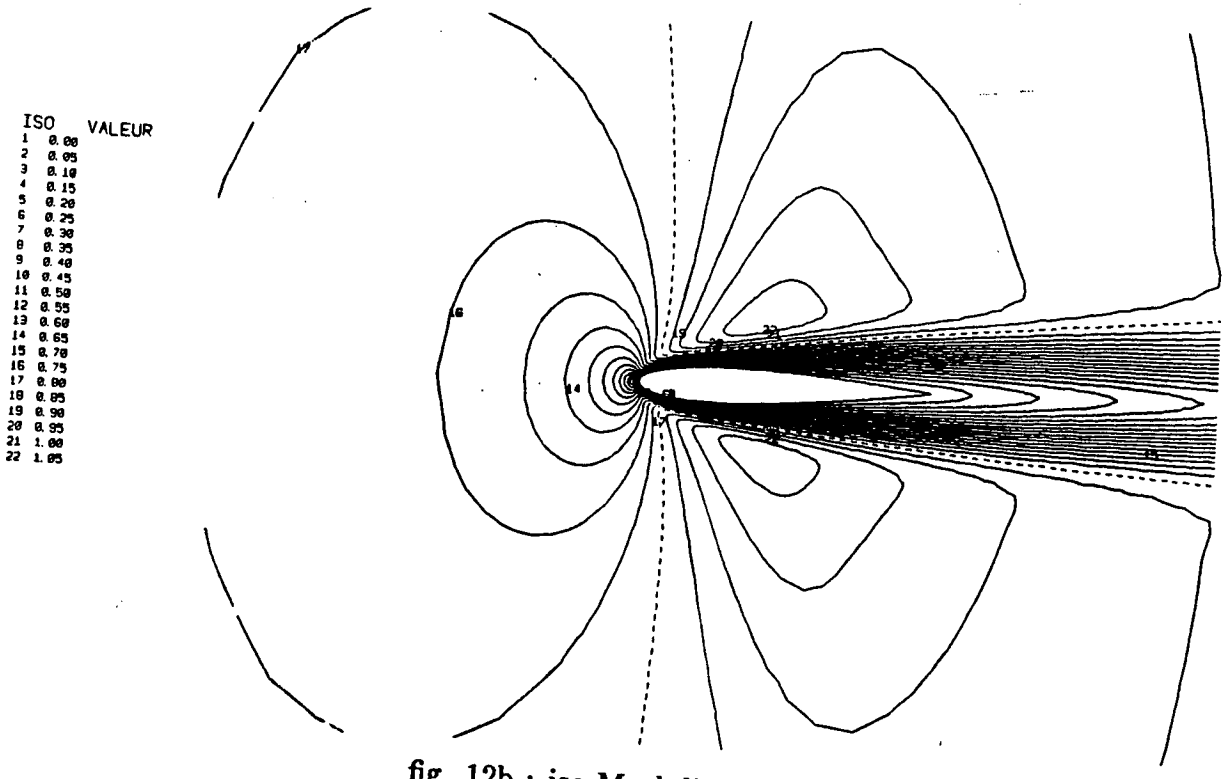

fig. 12b : iso Mach lines

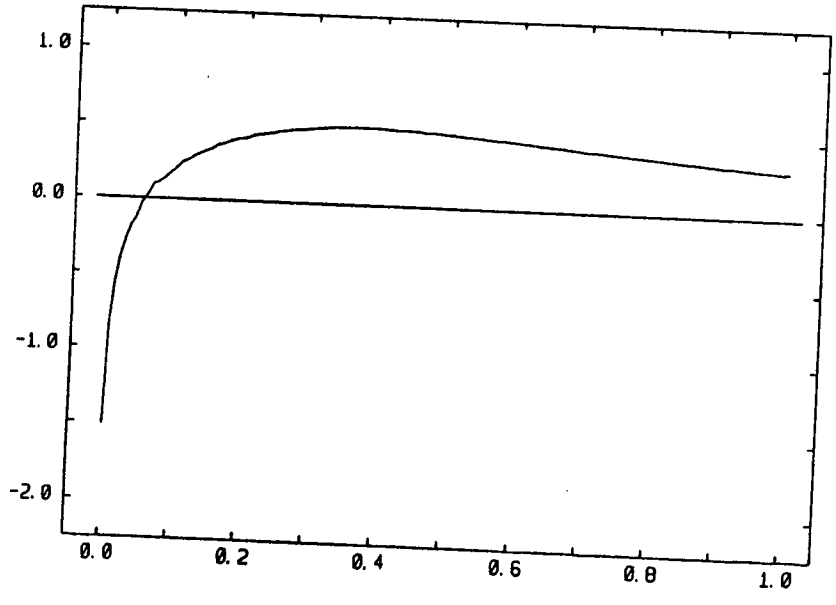

fig. 12c : pressure coefficient

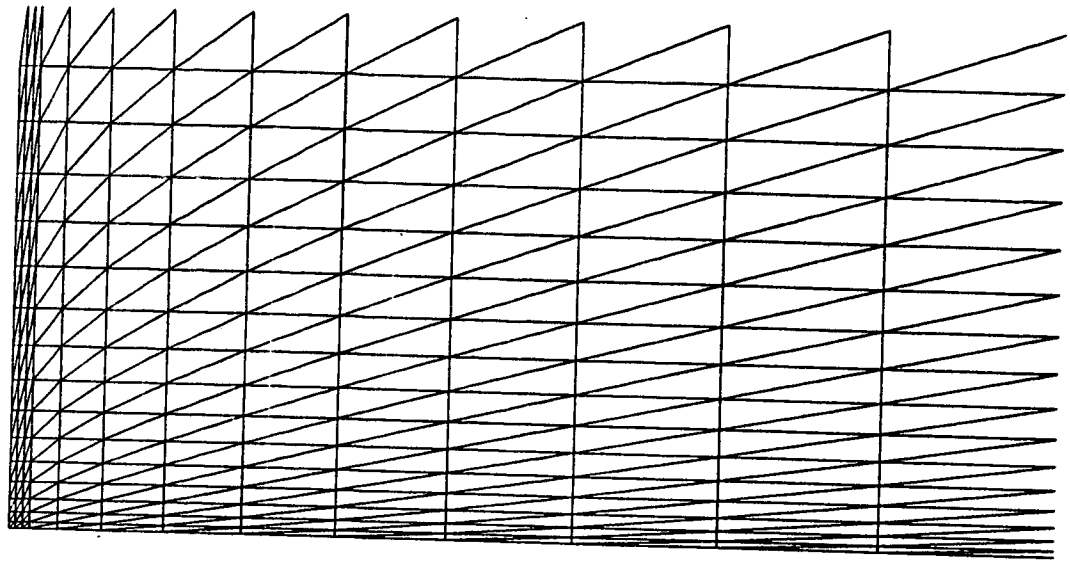

fig. 13a : mesh (partial view)

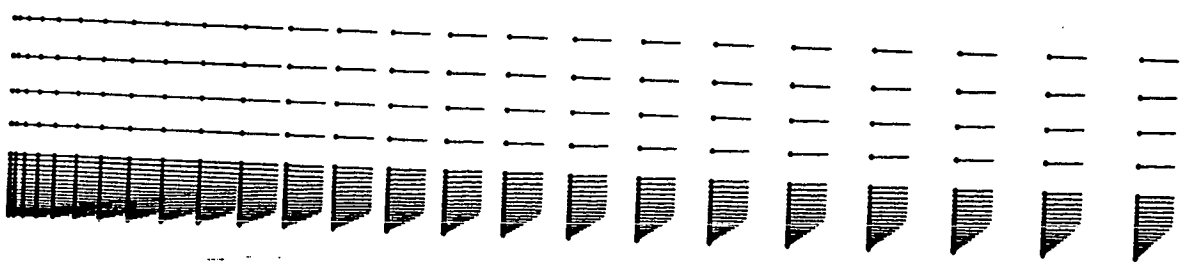

fig. 13b : speed vectors

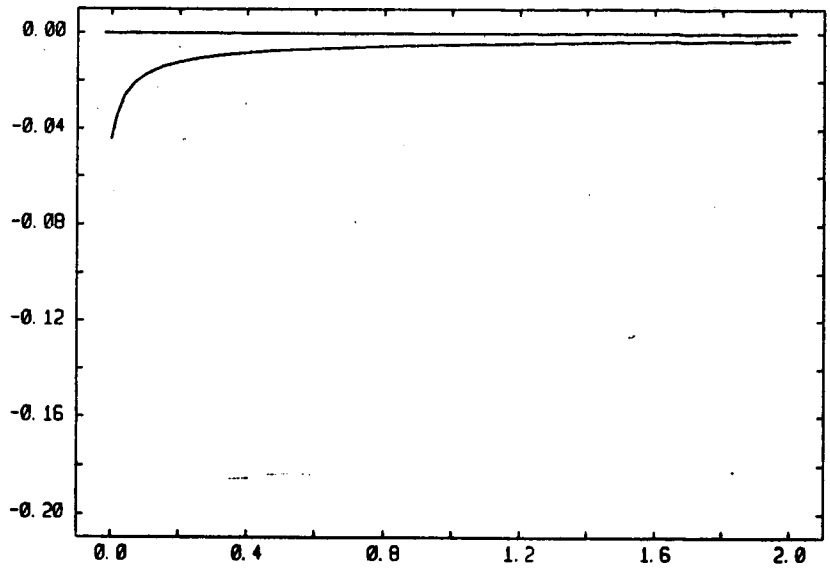

fig. 13c : pressure coefficient

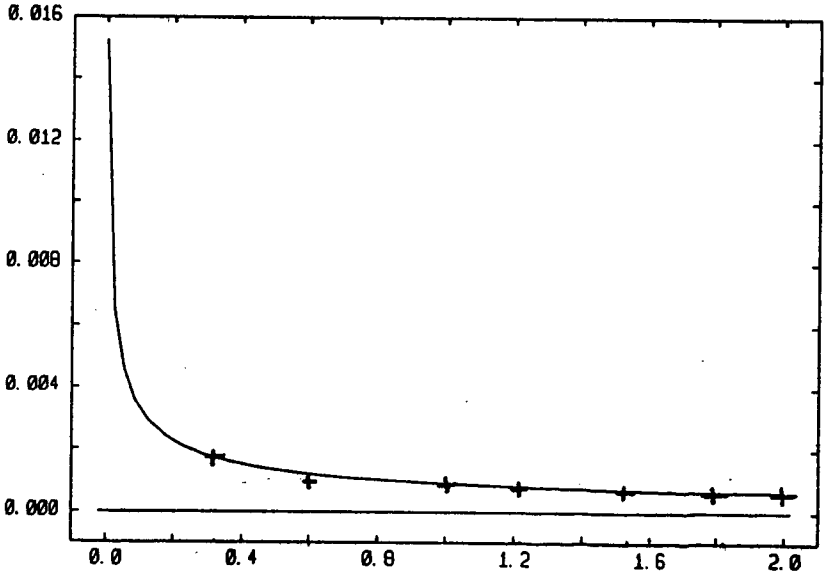

fig. 13d : skin friction coefficient

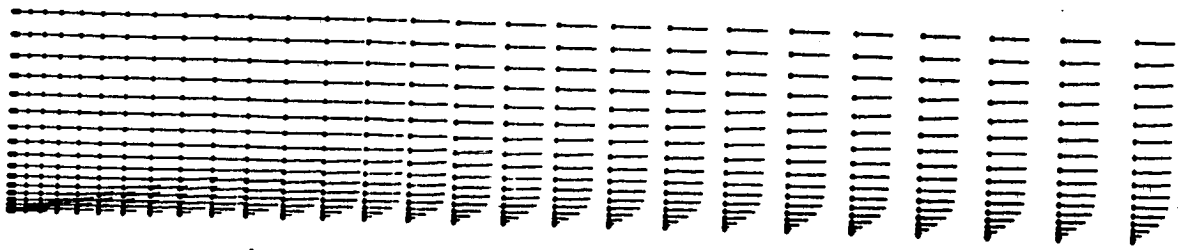

fig. 14 : speed vectors

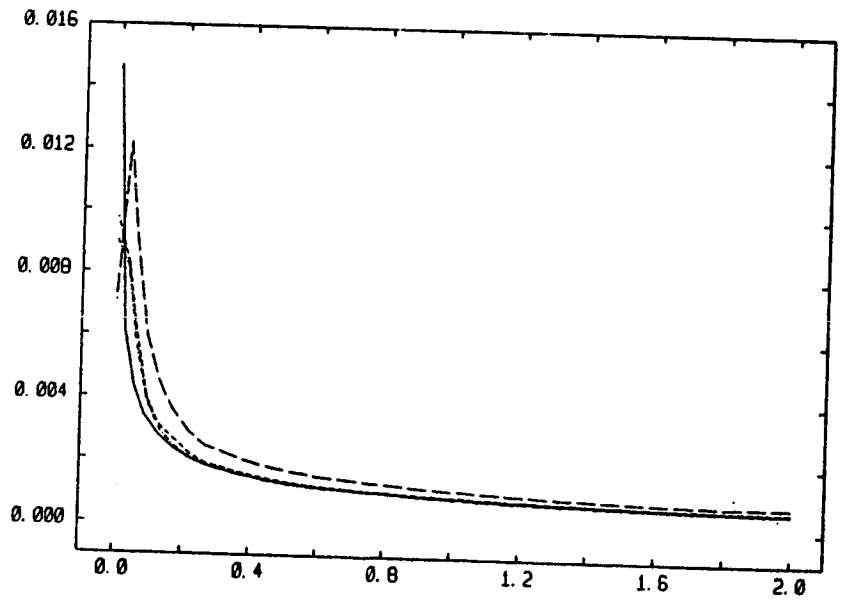

fig. 15 : comparison of skin friction for different limiters. Long broken: Van Albada limiter, short broken: third order extended ϕ limiter, broken dotted: κ limiter, full: reference result.

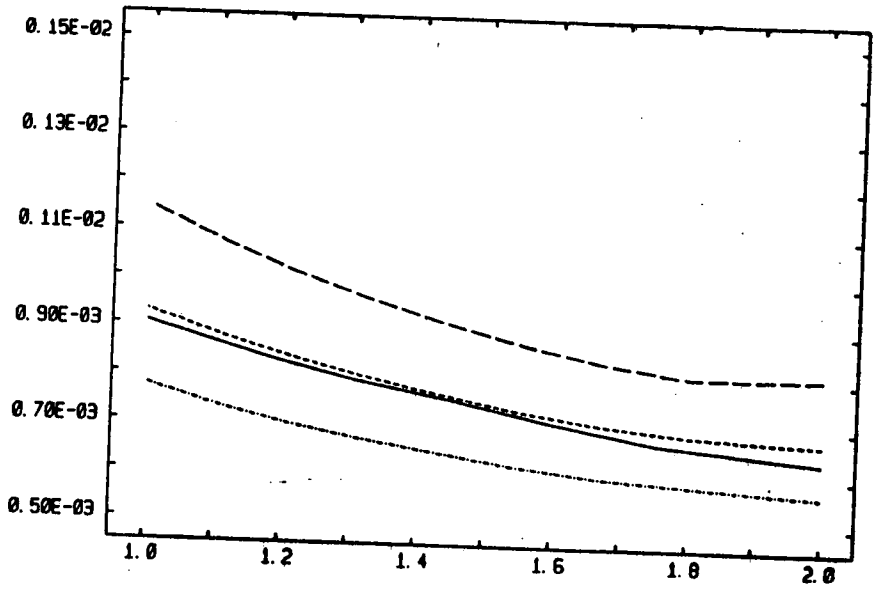

fig. 16a : comparison of skin friction for different limiters, enlargement. Long broken: Van Albada limiter, short broken: κ limiter, full: reference result, broken dotted: third order extended superbee .

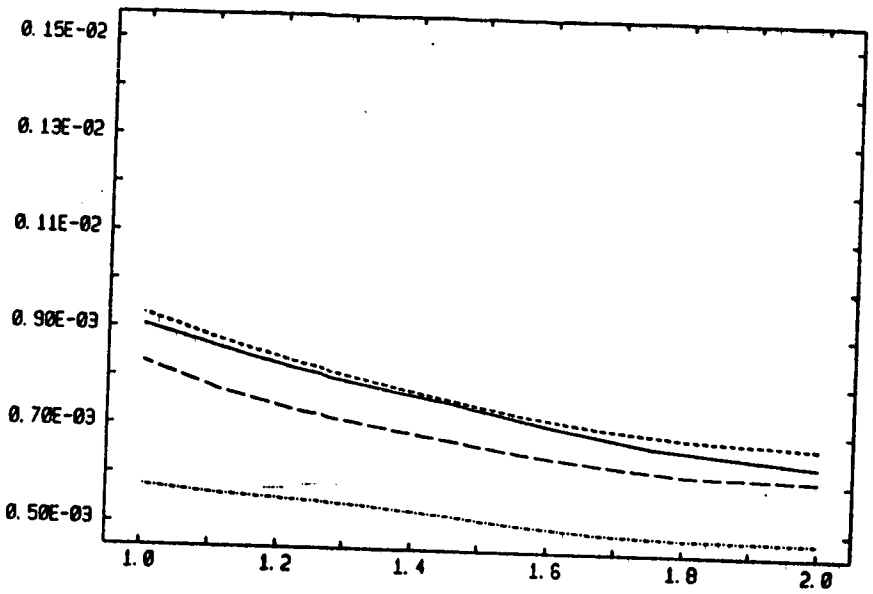

fig. 16b : comparison of skin friction for different limiters, enlargement. Long broken: extended ϕ limiter, short broken: κ limiter, full: reference result, broken dotted: extended superbee .

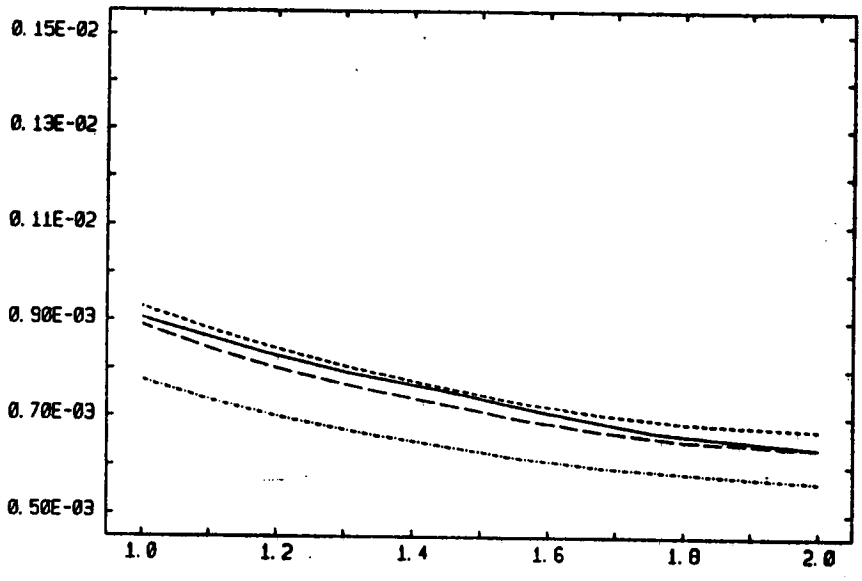

fig. 16c : comparison of skin friction for different limiters,
enlargement. Long broken: extended third order ϕ limiter,
short broken: κ limiter, full: reference result,
broken dotted: extended third order superbee .

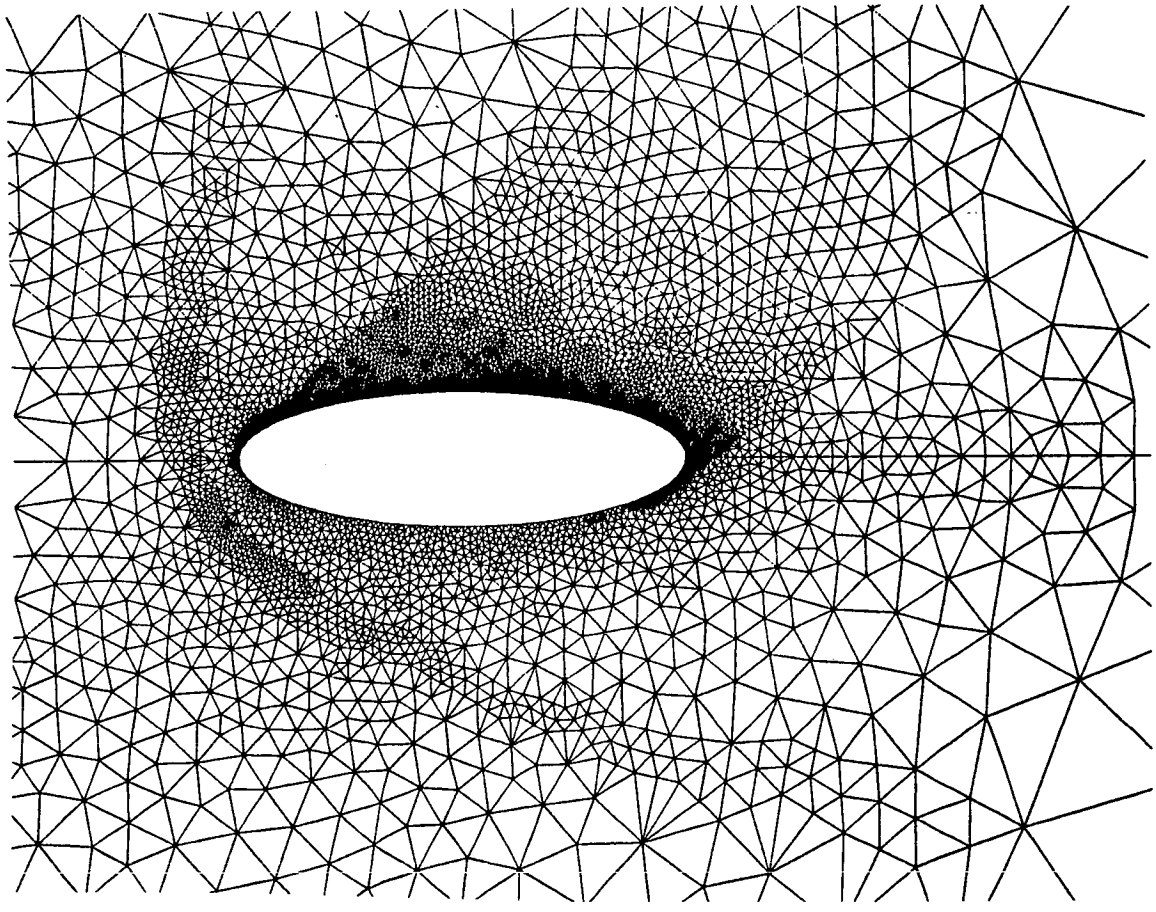

fig. 17a : 5172 Nodes, 9986 Elements (partial view)

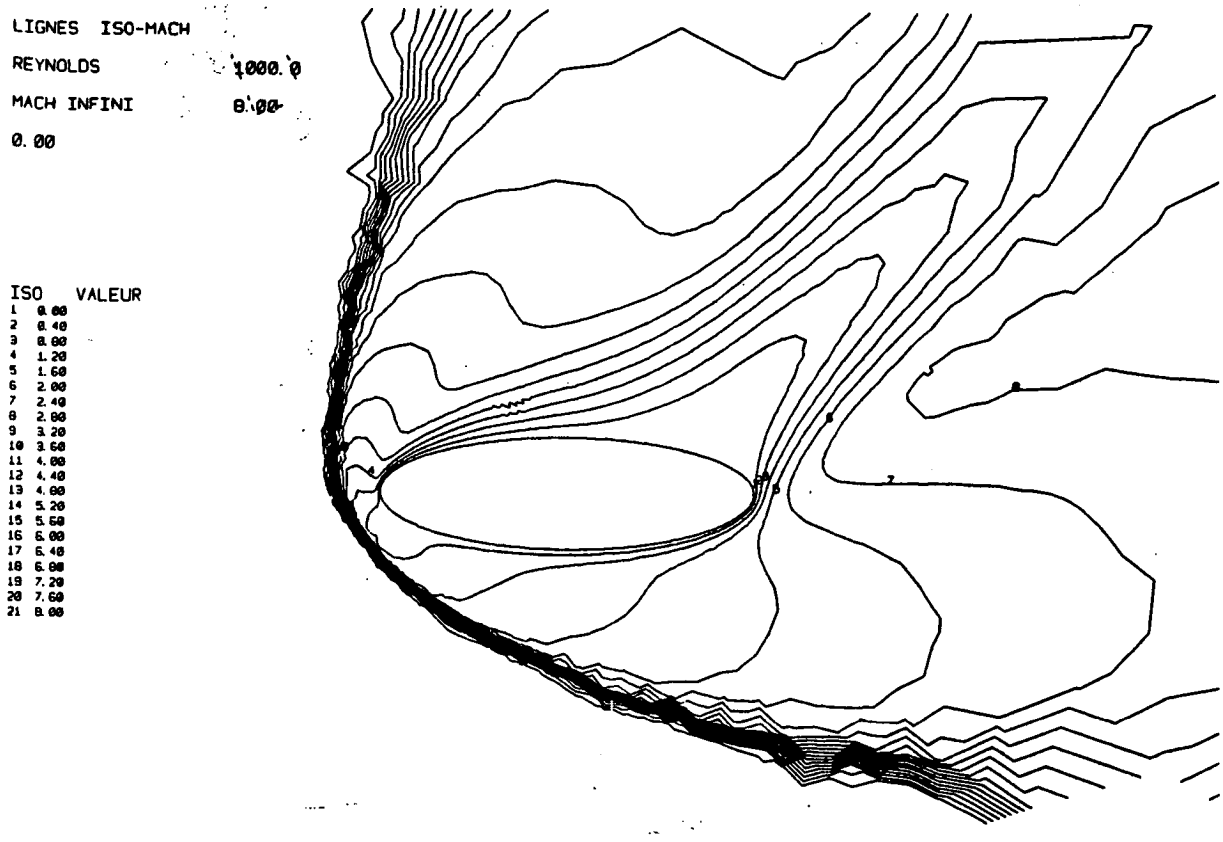

fig. 17b : iso Mach lines

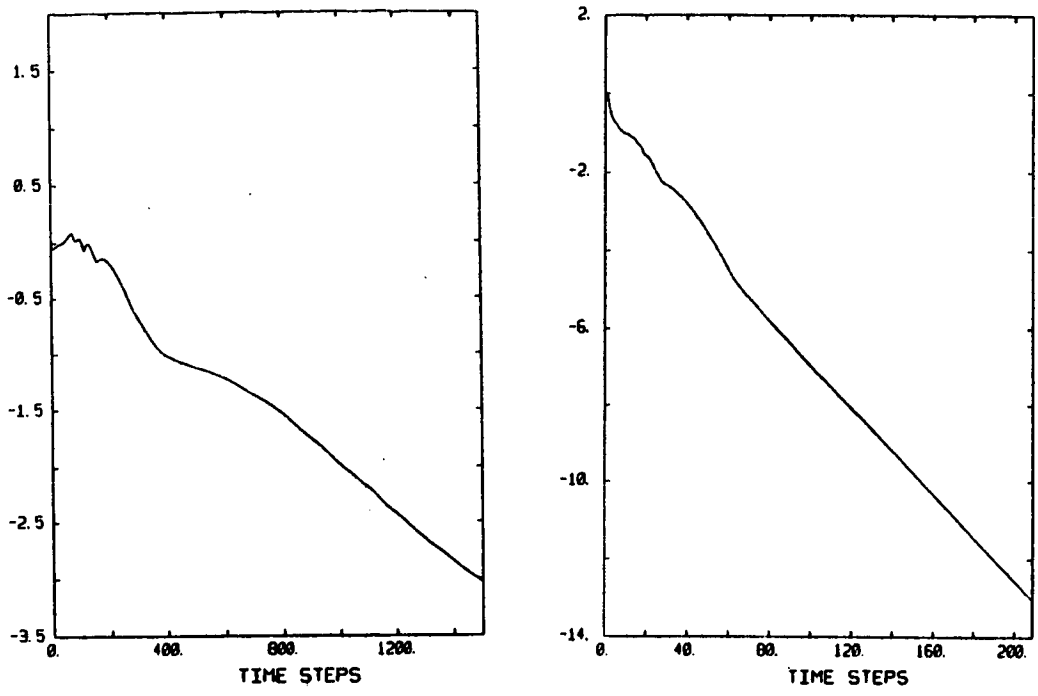

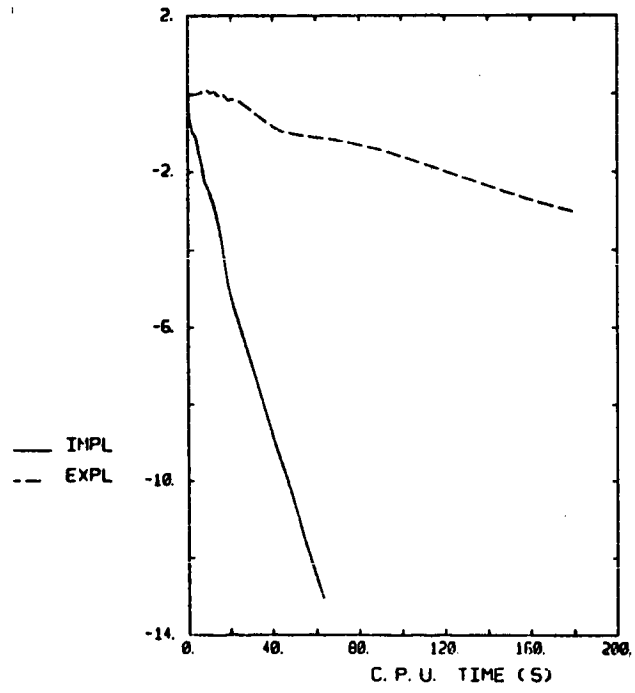

fig. 18

Imprimé en France
par
l'Institut National de Recherche en Informatique et en Automatique